



# Microarray Analysis of Cell Cycle Gene Expression in Adult Human Corneal Endothelial Cells

Binh Minh Ha Thi<sup>1</sup>, Nelly Campolmi<sup>1,2</sup>, Zhiguo He<sup>1</sup>, Aurélien Pipparelli<sup>1</sup>, Chloé Manissolle<sup>1</sup>, Jean-Yves Thuret<sup>4</sup>, Simone Piselli<sup>1</sup>, Fabien Forest<sup>1,3</sup>, Michel Peoc'h<sup>1,3</sup>, Olivier Garraud<sup>5</sup>, Philippe Gain<sup>1,2</sup>, Gilles Thuret<sup>1,2,6\*</sup>

**1** Laboratory for corneal graft biology, engineering and imaging<sup>1</sup>, EA2521, SFR143, Faculty of Medicine of the University Jean Monnet, Saint-Etienne, France, **2** Department of Ophthalmology, University Hospital, Saint-Etienne, France, **3** Department of Pathology, University Hospital, Saint-Etienne, France, **4** Service de Biologie Intégrative et de Génétique Moléculaire (SBIGeM), Institut de biologie et de technologies de Saclay (iBiTec-S), Commissariat à l'Energie Atomique, Gif-sur-Yvette, France, **5** Eye Bank, Etablissement Français du Sang Loire/Auvergne, Saint-Etienne, France, **6** Institut Universitaire de France, Paris, France

## Abstract

Corneal endothelial cells (ECs) form a monolayer that controls the hydration of the cornea and thus its transparency. Their almost nil proliferative status in humans is responsible, in several frequent diseases, for cell pool attrition that leads to irreversible corneal clouding. To screen for candidate genes involved in cell cycle arrest, we studied human ECs subjected to various environments thought to induce different proliferative profiles compared to ECs *in vivo*. Donor corneas (a few hours after death), organ-cultured (OC) corneas, *in vitro* confluent and non-confluent primary cultures, and an immortalized EC line were compared to healthy ECs retrieved in the first minutes of corneal grafts. Transcriptional profiles were compared using a cDNA array of 112 key genes of the cell cycle and analysed using Gene Ontology classification; cluster analysis and gene map presentation of the cell cycle regulation pathway were performed by GenMAPP. Results were validated using qRT-PCR on 11 selected genes. We found several transcripts of proteins implicated in cell cycle arrest and not previously reported in human ECs. Early G1-phase arrest effectors and multiple DNA damage-induced cell cycle arrest-associated transcripts were found *in vivo* and over-represented in OC and *in vitro* ECs. Though highly proliferative, immortalized ECs also exhibited overexpression of transcripts implicated in cell cycle arrest. These new effectors likely explain the stress-induced premature senescence that characterizes human adult ECs. They are potential targets for triggering and controlling EC proliferation with a view to increasing the cell pool of stored corneas or facilitating mass EC culture for bioengineered endothelial grafts.

**Citation:** Ha Thi BM, Campolmi N, He Z, Pipparelli A, Manissolle C, et al. (2014) Microarray Analysis of Cell Cycle Gene Expression in Adult Human Corneal Endothelial Cells. PLoS ONE 9(4): e94349. doi:10.1371/journal.pone.0094349

**Editor:** Irina Kerkis, Instituto Butantan, Brazil

**Received:** December 30, 2013; **Accepted:** March 13, 2014; **Published:** April 18, 2014

**Copyright:** © 2014 Ha Thi et al. This is an open-access article distributed under the terms of the Creative Commons Attribution License, which permits unrestricted use, distribution, and reproduction in any medium, provided the original author and source are credited.

**Funding:** Funded by Fondation de l'Avenir ET7-468, Agence de la Biomédecine 2013. The funders had no role in study design, data collection and analysis, decision to publish, or preparation of the manuscript.

**Competing Interests:** The authors have declared that no competing interests exist.

\* E-mail: gilles.thuret@univ-st-etienne.fr

## Introduction

The corneal endothelium, which maintains stable corneal transparency in humans, is essential to visual-system performance [1]. It is a monolayer of hexagonal, densely packed corneal endothelial cells (ECs) separating the corneal stroma from the aqueous humor. By actively regulating hydration of the stroma, it prevents the onset of edema which, by disorganizing the collagen fibrils, would impair the passage of light [2]. In humans, corneal ECs lose their proliferative ability during fetal development [3,4] and are consequently vulnerable *in vivo*. If the endothelium sustains a lesion, its integrity, which is necessary for its function, is only maintained by the migration and enlargement of the ECs adjacent to the lesion, without mitosis. As a result, when endothelial cell density (ECD) falls below a critical threshold (which depends on the type, extent and kinetics of the pathological process), irreversible corneal edema sets in. Endothelial diseases are a frequent cause of corneal blindness, for which only a corneal graft can restore vision. The graft, whether full thickness (penetrating keratoplasty, PKP) or endothelial (endothelial

keratoplasty, EK), supplies a new pool of functional ECs from the donor cornea. However, after both types of graft, ECD falls rapidly in the first 6 months, then more slowly, but at a higher rate than the physiological EC loss rate of 0.6% a year [5]. Recipients thus frequently need more than one graft during their lifetime.

The absence of corneal EC division is therefore responsible for significant corneal blindness worldwide. Knowing which cellular mechanisms are implicated in human corneal EC cycle arrest would thus allow the development of new therapeutic tools to trigger and control EC proliferation. *In vivo*, ECs are blocked in G1 phase but maintain a residual proliferative capacity that can be exploited *in vitro*. The senescent state of central ECs *in vivo* may result from many simultaneous mechanisms (exposed in [6,7,8]): low level of growth factors in aqueous humor, lack of autocrine stimulation by growth factors synthesized by ECs, cell cycle entry inhibition by TGF- $\beta$ 2 present in aqueous humor, contact inhibition induced by formation of mature cell-cell and cell-substrate junctions, oxidative DNA damage resulting in a permanently high level of mRNA or proteins of the cyclin-dependent kinase inhibitors (CDKI) p27, p21, and p16, and

cascades of blocking points for G1-S transition, especially belonging to the p53 pathway.

There are at least three possible areas of development for advanced therapy medicinal products in the field of ECs: 1/*Ex vivo* enrichment of grafts in EC is a realistic prospect [9] that would improve both the quality (prolonged survival in recipients) and the quantity of available graft tissue (by upgrading corneas whose ECD was initially too low). 2/*In vitro* mass culture of ECs would also allow bioengineering of endothelial graft tissue. 3/*In parallel*, it would become conceivable to treat early stages of primitive (Fuch's) or secondary endothelial dystrophies *in vivo* by injecting ECs in the anterior chamber [10]. Until now, three main approaches were used to trigger human EC proliferation (Table 1): 1/A general approach of improving culture conditions to limit cell death and promote cell cycle stimulating factors. 2/A focused approach focusing on a limited number of key cycle-controlling proteins considered as EC cycle blocking points. 3/Selecting and stimulating potential EC progenitor or stem cells located at the extreme periphery of the endothelium [11,12].

In the present study, we used a specific chip of 112 genes implicated in cell cycle regulation to examine human ECs subjected to six environments thought to induce different proliferative profiles: *in vivo*, post mortem (PM), organ culture (OC) stored corneas, confluent primary culture (CPC), non-confluent primary culture (NCPC), and immortalized EC line (ECL). We hypothesized that these six conditions form a coherent gradation from the well-recognized non-proliferative status of ECs *in vivo* to the immortalized ECs line that continuously proliferates, with four intermediate states liable to allow identification of differentially expressed genes. Unlike short-term cold storage, OC in fetal calf serum (FCS) supplemented medium maintains EC viability and functionality for up to 5 weeks. OC is not known to promote EC proliferation, although it facilitates endothelial wound healing by migration of cells in the vicinity of local defects in the endothelial layer [13]. Only OC with 8% FCS, a method that remains an exception [14], seems likely to promote cell mitosis [15]. It was thus important to determine whether routine OC induces significant transcriptional profile changes liable to reveal the stimulation of certain ECs with residual proliferative capacity. *In vitro*, primary cultures of ECs with FCS and growth factors usually have limited proliferative capacity and rapidly become senescent, especially when reaching confluence. Conversely, ECLs obtained by transducing simian virus 40 large T-antigen expression display very high proliferative capacity [16].

Hence, the crossing analysis of these models, from *in vivo* to the ECL, helps us to understand mechanisms implicated in EC division and senescence, thus giving new potential key points for triggering mitosis. Gottsch's major work on human endothelial cornea genomics proposed an analysis of all transcripts present in normal endothelia [17] and in Fuch's dystrophy [18] by using an ultra-sensitive SAGE method and Affymetrix HU95a microarrays containing about 12000 genes previously characterized in terms of function or disease association. In addition, Gottsch's team created a comprehensive database of human corneal gene expression. To date, no focused analysis has been done on the expression of genes implicated in cell cycle control in human ECs.

## Materials and Methods

### Ethics statement

All procedures conformed to the tenets of the Declaration of Helsinki for biomedical research involving human subjects. Central corneal buttons removed as waste during surgery were

collected as per the usual protocol in force in our University Hospital and by presumed consent further to the written information given to all admitted patients. This protocol was written by our Hospital's commission for clinical research and innovation and accepted by the local ethics committee (CPP Sud Est I, University Hospital, Saint Etienne, France). Corneas assigned to scientific use were procured from bodies donated to science (Laboratory of Anatomy, Faculty of Medicine) as permitted by French law. Each donor volunteers their body and gives written consent to the Laboratory of Anatomy; no extra specific approval by the ethics committee is required

### Materials

Serum-free medium (OptiMEM-1), Petri dish, 6-well tissue culture plates, T25 flasks and fetal bovine serum (FBS) were purchased from Fisher Bioblock Scientific (Vaulx-Milieu, France). Medium 199 (M199), epidermal growth factor (EGF; from mouse submaxillary glands), nerve growth factor (NGF; from mouse submaxillary glands), bovine pituitary extract (also known as Keratinocyte Growth Supplement), ascorbic acid, calcium chloride, chondroitin sulphate, 0.02% EDTA solution (EDTA disodium salt), antibiotic-antimycotic solution, gentamicin, trypsin, glutamine, penicillin-streptomycin solution, insulin and RNA loading dye were purchased from Sigma-Aldrich (Saint-Quentin Fallavier, France). Cell attachment reagent (FNC Coating Mix) was purchased from Gentaur (Brussels, Belgium). RNeasy mini Kit, RNase-free DNase I and Taq PCR Master Mix were purchased from Qiagen (Courtaboeuf, France). Oligo(dT)<sub>12-18</sub> primer, dNTP Mix (10 mM), Ribonuclease H, dithiothreitol (DTT; 0.1 M), 5× First-Strand Buffer, SuperScript II Reverse Transcriptase, Ribosomal protein S27a (RPS27A) forward and reverse primers were purchased from Invitrogen (Cergy Pontoise, France). Biotin-16-UTP was purchased from Roche Applied Science (Meylan, France). Cell Cycle OligoArray (Oligo GEArray Human Cell Cycle OHS-020) and Oligo GEArray Starter Kit (SABiosciences Corporation, SuperArray, Frederick, MD) were purchased from Tebu-bio (Le Perray en Yvelines, France). Inventoried TaqMan Gene Expression Assays and TaqMan Universal PCR Master Mix were purchased from Applied Biosystems (Courtaboeuf, France).

### Human corneal tissue

In order to study ECs in the physiological *in vivo* state as closely as possible, ECs from patients undergoing corneal graft for keratoconus were chosen. Keratoconus is a common non-inflammatory, progressive disease in which the endothelial layer is healthy and not known to be involved in the disease pathogenesis. Penetrating keratoplasty consists of replacing the central full-thickness cornea by a normal donor cornea. Consequently, a normal endothelium can be obtained during surgery. Eight central corneas (diameter 8.25 mm) were obtained during penetrating grafts for keratoconus, immediately after trephination (*in vivo* group). ECs were collected as explained above. Time from trephination to endothelial freezing was about 20 minutes. Thirty-four supplementary human corneas assigned to scientific use (procured from bodies donated to science) were used in this study. Donor and procurement characteristics are presented in Table 2. Except for the *in vivo* group, corneas were procured by a 16–18 mm diameter *in situ* excision, as per the procedure recommended in France for corneas intended for transplantation. Twelve corneas, forming the post-mortem group, were immediately used. Eleven corneas, forming the OC group, were immediately placed in 100 mL of OC medium (Corneamax®, Eurobio, Les Ulis, France) at 31°C in a dry incubator. Five

**Table 1.** Published experimental methods for triggering human corneal endothelial cell proliferation.

| Approach   | Principle  | Biological model  | Author, year   |
|--|--|---|--|
| FOCUSED  | Immortalization of primary HCEC  | Transduction of <b>simian virus 40 large T-antigen</b> expression   | human (in vitro) Wilson 1993 [92], Feldman 1993 [93] |
|  |  | Transformation with papillomavirus <b>E6/E7</b> oncogenes   | human (in vitro) Wilson 1995 [94]                    |
|  |  | Retroviral transduction of <b>Cdk4R24C/CyclinD1</b> to human corneal endothelial  | human (in vitro) Yokoi 2012 [75]                     |
|  |  | Transduction of human <b>telomerase reverse transcriptase expression</b> (hTERT)  | human (in vitro) Liu 2012 [95]                       |
|  |  | Transduction of <b>hTERT</b> combined with <b>p53</b> downregulation or <b>CDK4</b> overexpression  | human (in vitro) Sheerin 2012 [8]                    |
|  | E2F2 overexpression  | Transduction of <b>E2F2</b>   | human (ex vivo) McAlister 2005 [96]                  |
|  | CDKI down regulation   | siRNA <b>p27Kip1</b>  | human (in vitro) Kikuchi 2006 [25]                   |
|  |  | Electroporation with <b>p21+p16</b> siRNA   | human (in vitro) Joyce 2010 [97]                     |
|  | Anti-apoptotic effect  | Transduction of baculoviral <b>p35</b> or mammalian <b>Bcl-xL</b> for anti-apoptotic gene therapy   | human (in vitro) Fuchsluger 2011 [98]                |
|  | GENERAL  | Medium optimization   | Organ culture at 32°C with 8% FCS                    |
| Evaluation of 4 basic culture <b>medias</b> (DMEM, OptiMEM-I, DMEM/F12, Ham's F12/M199) in isolation & propagation |  |   | human (in vitro) Peh 2011 [99]                       |
| Reduction of reactive oxygen species by <b>rapamycin &amp; cysteamine</b>  |  |   | human (in vitro) Shin 2012 [100]                     |
| Culture support  |  | <b>Decellularized bovine corneal posterior lamellae</b> as carrier matrix for cultivated cells  | human & bovin (ex vivo, in vitro) Bayyoud 2012 [101] |
|  |  | <b>Gelatin hydrogel carrier</b> sheet for corneal endothelial transplantation.  | human (in vitro) Watanabe 2011 [102]                 |
| Cell-cell contact release  |  | <b>EDTA</b> +organ culture at 37°C+10% FCS <sup>†</sup> , 10 ng/mL EGF <sup>†</sup> , 20 ng/mL FGF <sup>†</sup>   | human (ex vivo) Senoo 2000 [103], Patel 2009 [104]   |
|  | <b>Localized lesion</b> +organ culture at 37°C+10% FCS <sup>†</sup> , 10 ng/mL EGF <sup>†</sup> , 20 ng/mL bFGF <sup>†</sup> | human (ex vivo) Senoo, 2000 [105]   |  |
| REGENERATION   | HCEC precursor   | Isolation of <b>HCEC precursors</b> in vitro by sphere-forming assay  | human (in vitro) Yokoo 2005 [106]                    |
|  | Stromal cornea-derived precursors  | Differentiation of <b>stromal cornea-derived precursors</b> to functional corneal endothelium by cell isolation in medium containing retinoic acid, GSK 3b inhibitor and Rock inhibitor Y-27632 | human (in vitro) Hatou 2012 [107]                    |
|  | Trabecular meshwork stem-like cell   | Local progenitors for the corneal endothelium and <b>trabecular meshwork</b> personalized stem cell therapy in corneal endothelial diseases and glaucoma (Review)                               | / Yu 2012 [108]                                      |

<sup>†</sup>FCS: Foetal calf serum; EGF: Epidermal growth factor; FGF: Fibroblast growth factor.  
doi:10.1371/journal.pone.0094349.t001

corneas were used to carry out confluent primary culture (CPC group). The last six corneas were used to carry out non-confluent primary culture (NCPC group). SV40 immortalized ECs

(HCECT-12) were bought from DMSZ (Braunschweig, Germany) [16,19] and are henceforth referred to as the endothelial cell line (ECL).

**Table 2.** Characteristics of donor corneas.

| Condition                     | Biological replicate | Age (years) | Death/retrieval time (hours) | Storage time (days) |
|-------------------------------|----------------------|-------------|------------------------------|---------------------|
| In vivo                       | 15                   | 44 (27–81)  | /                            | /                   |
| Post-mortem                   | 12                   | 79 (49–98)  | 12 h25 (4 h–21 h45)          | /                   |
| Organ culture                 | 11                   | 69 (49–85)  | 11 h40 (5 h30–15 h55)        | 16 (13–24)          |
| Confluent primary culture     | 5                    | 78 (65–88)  | 13 h08 (6 h30–21 h25)        | 13 (8–18)           |
| Non-confluent primary culture | 6                    | 78 (58–89)  | 15 h26 (11 h–16 h30)         | 21 (4–48)           |

Values were expressed as median (min-max).  
doi:10.1371/journal.pone.0094349.t002

## Cell culture

**Primary culture.** ECs were isolated and cultured according to published protocols [20,21,22,23,24,25]. Briefly, Descemet membrane and ECs were peeled off under an operating microscope and separated into small fragments that were immersed in culture medium containing OptiMEM-I, 10% FBS, 5 ng/mL EGF, 20 ng/mL NGF, 100 µg/mL pituitary extract, 20 µg/mL ascorbic acid, 200 mg/L calcium chloride, 0.08% chondroitin sulphate, 50 µg/mL gentamicin, and antibiotic/antimycotic solution diluted 1/100. Isolated cells and pieces of Descemet membrane that still contained attached cells were plated in six-well tissue culture plates precoated with undiluted FNC Coating Mix. Cultures were then incubated at 37°C in a 5% carbon dioxide, humidified atmosphere. Medium was changed every 2 days. Confluent primary cultured cells were then trypsinized, resuspended in culture medium, and subcultured into T25 flasks that had been precoated and grown to 50% or 100% confluence.

**Immortalized cell line.** The ECL was cultured as previously described [26] with some technical changes. Briefly, cells were grown in T25 flasks with culture medium F99 (1:2 dilution of medium 199 and Ham's F12) supplemented with 0.3% chondroitin sulphate, 2% glutamine, 0.5% penicillin-streptomycin solution, 0.02% ascorbic acid, 0.02% insulin and 10% FCS. The cultures were maintained in 5% CO<sub>2</sub> at 37°C. Culture medium was changed every 2–3 days.

## RNA extraction

Under an operating microscope, Descemet membrane with endothelium was peeled off from the underlying stroma with forceps to avoid contamination by other cell types. Two corneas were pooled for the OC and post-mortem groups (whole cornea), and four for the in vivo group (8 mm diameter trephination). Microarrays were consequently performed in duplicate for each condition. This approach minimizes inter individual differences and was extensively published [27,28,29]. Non-confluent and confluent primary cultures and ECL cultures were trypsinized and pelleted. Descemet membrane fragments and ECs were then frozen at –80°C until RNA isolation. Total RNA was isolated using an RNeasy mini kit as per the manufacturer's instructions. Before further use, total RNA was treated with RNase-free DNase I [30]. After extraction, RNA was checked for stability and DNA contamination by running a sample with an RNA loading dye on a 1% agarose gel, and visualization was done by staining with ethidium bromide. Lack of genomic DNA contamination was confirmed by polymerase chain reaction (PCR) amplification of RNA samples that had not been reverse-transcribed. RNA quantity was determined by spectrophotometric absorbance of the sample at 260 nm measurement, and purity was determined based on the ratio at 260 nm to that of 280 nm ( $A_{260}/A_{280}$ ) using a BioMate 3 Series spectrophotometer (Thermo Fisher Scientific, Cergy Pontoise, France). Only RNA samples with  $A_{260}/A_{280}$  ratio >1.8 were used for further experiments. Samples were frozen at –80°C until use in microarrays and qRT-PCR.

## Polymerase chain reaction

PCR was carried out on RNA of each sample in order to check possible contamination with genomic DNA. Amplification was performed by the standard method on Ribosomal protein S27a (RPS27A) gene using Taq PCR Master Mix as per the manufacturer's instructions. RPS27A is a component of the 40S subunit of the ribosome, and has been previously identified as a valid control gene in expression studies conducted among human malignant and control tissues [31,32]. PCRs were performed in

100 µl reactions using 300 ng RNA, 2.5 units of Taq DNA Polymerase, 1× PCR Buffer (containing 1.5 mM MgCl<sub>2</sub>), 200 µM of each dNTP and 0.5 µM of each primer. The sequences of human RPS27A primers, described elsewhere [33,34], were as follows: forward primer, 5'-TCGTGGTGGTGCCTAAGAAA-3'; and reverse primer, 5'-TCTCGACGAAGGCGACTAAT-3'. Amplifications were carried out using the following cycling parameters: initial denaturation at 95°C for 10 minutes, denaturation at 95°C for 60 seconds, annealing at 53°C for 60 seconds, and extension at 72°C for 60 seconds. PCR amplification was done for 40 cycles with a final extension at 72°C for 10 minutes. RPS27A cDNA from cell line, obtained after RT, was used as a positive control. For a negative control, PCR was run using PCR reaction mixture with primers but no nucleic acid. Following amplification, the PCR products were characterized in 1% agarose-ethidium bromide gels in Trisacetate buffer. A product was obtained from PCR performed on positive control but not on RNAs and negative control, indicating that samples were not contaminated by genomic DNA (data not shown).

## Reverse transcription

First-strand cDNA synthesis was carried out on 300 ng of total RNA in a final volume of 20 µl with SuperScript II Reverse Transcriptase as per the manufacturer's protocol. Briefly, after addition in nuclease-free microcentrifuge tubes of 300 ng of total RNA, 0.1 µl Oligo(dT)<sub>12–18</sub> (500 µg/ml), 1 µl dNTP Mix (10 mM each) and sterile distilled water to complete the volume at 12 µl, the mixture was heated at 65°C for 5 minutes. 4 µl of 5× First-Strand Buffer and 2 µl of DTT were then added and the mix incubated at 42°C for 2 minutes. Incubation at 42°C for 50 minutes was performed after the addition of 1 µl of SuperScript II RT. The reaction was inactivated by heating at 70°C for 15 minutes. To remove RNA complementary to the cDNA, 1 µl of *E. coli* RNase H (two units) was added and the mixture incubated at 37°C for 20 minutes and then chilled on ice. cDNA were stored at –20°C until use in qPCR.

## GEArray

Expression levels of cell cycle-specific genes were examined by human cell cycle Oligo GEArray (OHS-020). The Oligo GEArray Human cell cycle Microarray profiled the expression of 112 key genes involved in cell cycle regulation, such as cyclin-dependent kinases (CDKs) involved in cell cycle progression and the proteins that regulate them (cyclins, CDK inhibitors, CDK phosphatases and kinases). Genes essential for DNA damage and mitotic spindle checkpoints and genes in the SCF (*CUL1*, *SKP2*) and APC (anaphase promoting complex, with *CDC16-20*, *ANAPC2-4-5*) ubiquitin-conjugation complexes were also included. Microarrays were performed in two biological replicates for each group. Briefly, as described elsewhere [35,36,37,38,39], using the TrueLabeling-AMP 2.0 kit, 1 µg of purified total RNA was reversely transcribed to obtain cDNA and converted into biotin-labeled cRNA using biotin-16-UTP (Roche) by in vitro transcription. The biotin-labeled cRNA was purified using the cRNA clean-up kit. Prehybridization (2 hours) and hybridization (overnight) was done at 60°C in a hybridization oven using 3 µg purified labeled cRNA target as per manufacturer's protocol. After washing and blocking the array membranes, alkaline phosphatase-conjugated streptavidin was allowed to bind and CDP-Star substrate chemiluminescence was detected by exposure to x-ray film. The film was acquired using a 16-bit desktop scanner and saved as a grayscale 16-bit TIFF file. Absence of signal saturation (number of grey levels <255) was verified for each image. Array data were analyzed using the web-based GEArray Expression Analysis Suite

**Table 3.** TaqMan gene expression assays for quantitative real-time PCR used to validate microarray results on a subset of 11 genes of interest.

| Assay ID      | NCBI Gene Reference | Gene Symbol    | Gene Name  | Target Exons | Amplicon Length |
|---------------|---------------------|----------------|--|--------------|-----------------|
| Hs01026536_m1 | NM_001238.1         | <i>CCNE1</i>   | Cyclin E1  | 11–12        | 64              |
| Hs00277039_m1 | NM_053056.2         | <i>CCND1</i>   | Cyclin D1  | 2–3          | 94              |
| Hs00696862_m1 | NM_002592.2         | <i>PCNA</i>    | Proliferating cell nuclear antigen                           | 1–2          | 95              |
| Hs01032443_m1 | NM_002417.4         | <i>MKI67</i>   | Antigen identified by monoclonal antibody Ki-67              | 8–9          | 66              |
| Hs00190723_m1 | NM_004675.2         | <i>DIRAS3</i>  | DIRAS family, GTP-binding RAS-like 3                         | 1–2          | 115             |
| Hs00169255_m1 | NM_001199741.1      | <i>GADD45A</i> | Growth arrest and DNA-damage-inducible, alpha                | 2–3          | 123             |
|               | NM_001924.3         |                |  | 3–4          | 123             |
| Hs00355782_m1 | NM_078467.1         | <i>CDKN1A</i>  | Cyclin-dependent kinase inhibitor 1A (p21 <sup>CIP1</sup> )  | 2–3          | 66              |
| Hs00153277_m1 | NM_004064.3         | <i>CDKN1B</i>  | Cyclin-dependent kinase inhibitor 1B (p27 <sup>KIP1</sup> )  | 1–2          | 71              |
| Hs00233365_m1 | NM_058195.2         | <i>CDKN2A</i>  | Cyclin-dependent kinase inhibitor 2A (p16 <sup>Ink4A</sup> ) | 2–3          | 117             |
| Hs00365249_m1 | NM_078487.2         | <i>CDKN2B</i>  | Cyclin-dependent kinase inhibitor 2B (p15 <sup>Ink4B</sup> ) | 1–2          | 128             |
| Hs00269187_m1 | NM_003592.2         | <i>CUL1</i>    | Cullin 1   | 2–3          | 165             |
| Hs99999901_s1 | X03205.1            | <i>18S</i>     | Eukaryotic 18S rRNA (Endogenous Controls)                    | —            | 187             |

doi:10.1371/journal.pone.0094349.t003

software (SuperArray Bioscience). All signal intensities were background subtracted (subtraction of minimum value), and normalized to the housekeeping genes (RPS27A; GAPDH; B2M; HSP90AB1 and ACTB). For each set of duplicates, the mean value for each gene was determined and used to calculate the fold-changes: the *in vivo* group served as reference sample. The cut-off induction determining expression was  $\geq 1.5$  fold changes [40,41,42], (fold change = normalized result of groups/normalized result of the control group). Genes suiting both the above criteria were considered to be upregulated or downregulated with biological relevance. To gather reliable data, careful quality control of experiments, data extraction and standardization approaches were maintained throughout the experimental process.

**Gene ontology (GO) and cluster analysis.** The enriched biological processes GO terms for each cell cycle phase was determined by uploading the gene list on the Database for Annotation, Visualization, and Integrated Discovery (DAVID) version 6.7, 2013 (<http://david.abcc.ncifcrf.gov/> [43,44], (Table S1 in File S1). Clustering of genes expression by cell cycle phase was conducted with the software R version 2.15.0, 2012 [45]. The fold-change expression values were represented in logarithmic scale in heatmap graph.

**Pathway profile analysis.** Gene Map Annotator and Pathway Profiler (GenMAPP) version 2.1 was used to analyze GEArrays results. Fold-change expression values of each biological group versus the *in vivo* group were related to the Kyoto Encyclopedia of Genes and Genomes (KEGG) pathway of human cell cycle [46,47]. Fold-change absolute values over 1.5 were considered as upregulated or downregulated and classified in three classes: 1.5 to 5 folds, 5 to 10 folds, and 10 folds and more.

### Real-time quantitative PCR

To confirm the cDNA arrays findings, real-time quantitative PCR were carried out on 11 selected genes: Cyclin D1; Cyclin E1; p21; p27; p16; p15; GADD45A, DIRAS3, cullin 1, MKI67 and PCNA using an AB 7500 Fast Real-Time PCR System (Applied Biosystems). Assays were performed with TaqMan Universal PCR Master Mix and Inventoried Taqman Gene Expression Assays (Table 3) as per the manufacturer's instructions. Briefly, in wells of a 0.2 ml optical-grade 96-well PCR plate, we placed a 25  $\mu$ l reaction mixture of 12.5  $\mu$ l TaqMan Universal PCR Master Mix, 900 nM of each unlabeled primers (forward and reverse), 250 nM TaqMan MGB (minor groove binder) probe and 25 ng cDNA for each of the target genes. The assay's probes incorporated a 5' reporter dye (6-carboxy-fluorescein, 6-FAM<sup>TM</sup> dye label) and a 3' non-fluorescent quencher (NFQ) and spanned an exon junction (Table 3); genomic DNA could not be detected. The thermal cycle conditions, as previously described [48] and as per the manufacturer's instructions, consisted of AmpErase activation (50°C, 2 min) and Taq activation (95°C, 10 min), followed by 40 cycles of denaturation (95°C, 15 sec), annealing and elongation (60°C, 1 min). The AB 7500 system measures a fluorescent accumulation of PCR product by continuous monitoring. 18S rRNA was used as an endogenous control to normalize for variation in the amount of cDNA template. Each sample also consisted of two biological replicates and three technical replicates. No Template Controls (NTC: PCR mixture without cDNA) were performed to rule out cross contamination of reagents, on each target as well as on endogenous control. All data were analyzed using the 7500 Fast System Detection Software version 1.2.3 (Applied Biosystems). After normalization of measurements using the endogenous control, results were analyzed using the comparative critical threshold ( $\Delta\Delta C_T$ ) method [49,50,51] to compare differences

between samples. As for the microarray, the *in vivo* group served as reference.

**Statistical analysis**

Spearman’s correlation coefficient (*r*) was calculated between the biological replicate of each group studied by microarray, in order to estimate reproducibility, and between microarray and qRT-PCR results to estimate the reliability of microarrays. *P* < 0.05 was considered statistically significant.

**Results**

**Gene expression profiles in endothelial cells from different environments**

Detection of cell cycle gene transcripts by GEMarray was successful for the six types of EC (Fig. 1). For each EC type, normalized values of biological duplicates were concordant with

Spearman’s correlation coefficients between biological replicates respectively of 0.891 for *in vivo*, 0.881 for PM, 0.972 for OC, 0.974 for CPC, 0.792 for NCPC, and 0.981 for the ECL (*p* < 0.001 for each).

Using cluster analysis of normalized values of the 112 cell cycle gene expressions, the heatmap representation (Fig. 2) exhibited the highest similarity between cell cycle gene expression of EC *in vivo* and PM. Samples collected from donors with short death to retrieval time (under 24 h) still had the same properties as the *in vivo* samples. OC shares similar patterns of expression with CPC and NCPC. The ECL clearly had a completely different profile, with activation of most cell cycle genes, and could consequently be considered a positive control for EC proliferation.

Based on GO classification, 62 of 112 genes analyzed by GEMarray were directly classified in cell cycle phases and checkpoints; 40 other genes were not classified. The percentage of genes over- or underexpressed is presented in Figure 3. In ex

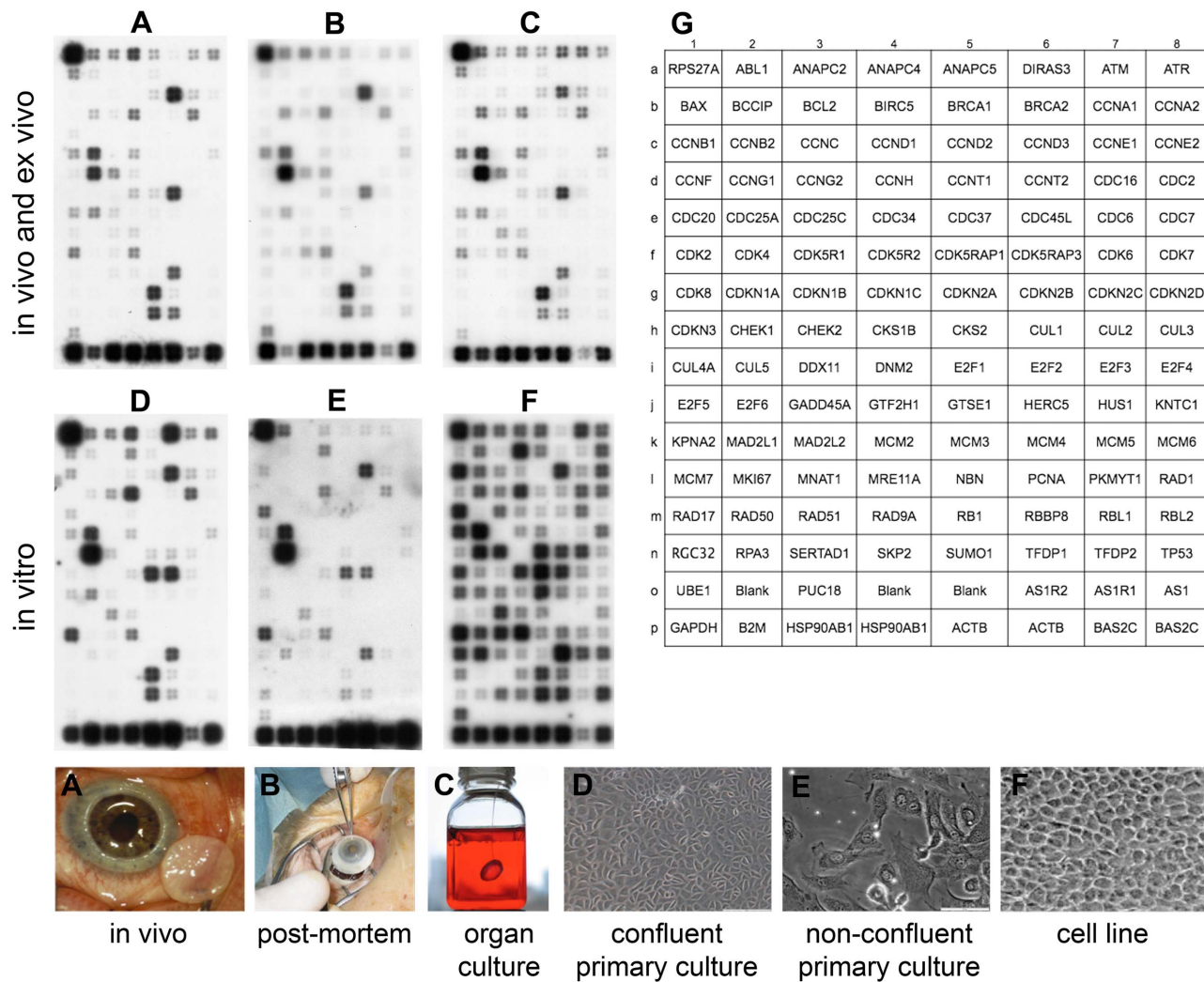


**Figure 1. Microarray analysis of mRNA extracted from endothelial cells collected on six biological models. (A)** *in vivo* corneas (reference group); **(B)** post-mortem corneas; **(C)** organ-cultured corneas; **(D)** confluent primary culture; **(E)** non-confluent primary culture; and **(F)** *in vitro* confluent cell line. Genes expressed were identified as a specific hybridization signal that appeared as tetra-spots. In addition to the 112 genes of interest, each chip contained five housekeeping genes for normalization (GADPH, beta-2-microglobuline (B2M), 2× HSP90AB1, 2× Actin beta (ACTB)), seven negative controls: PUC18 plasmid DNA, Artificial Sequence 1 related 2 (AS1R2), Artificial Sequence 1 Related 1 (AS1R1), Artificial Sequence 1 (AS1) and three blank spots, and two positive detection controls: two biotinylated Artificial Sequence 2 Complementary sequence (BAS2C) at increasing gradient. A key to gene coordinates is shown in panel **G**. doi:10.1371/journal.pone.0094349.g001

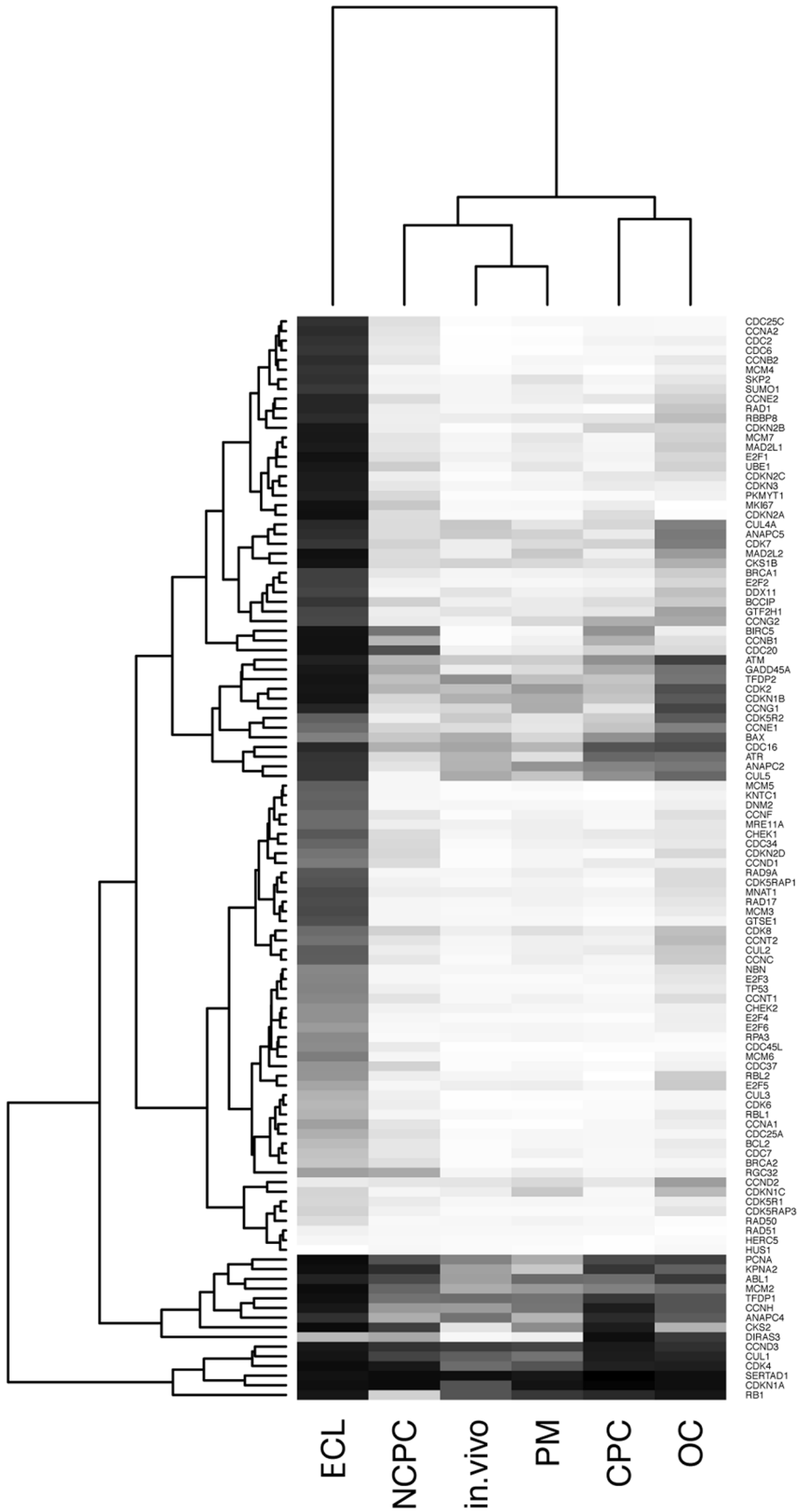


**Figure 2. Clustergram analysis of expression of 112 cell cycle genes in endothelial cells of the six different biological models: in vivo, post mortem (PM), organ culture (OC), in vitro confluent primary culture (CPC), in vitro non confluent primary culture (NCPC), and cell line (ECL).** Normalized expressions of all models were represented on the heatmap graph. Gray scale from 0 (blank) to 1 (black) represents variation between minimum and maximum normalized values.  
doi:10.1371/journal.pone.0094349.g002

vivo EC, compared to in vivo, cell cycle regulator genes were overexpressed progressively in PM and OC conditions. In isolated culture of EC, NCPC overexpressed cell cycle regulators compared to EC in CPC. Immortalized ECs overexpressed 100% of cell cycle regulators. Taken together, this general evaluation showed slight activation of the cell cycle in ECs of corneas shortly after donors' death, and high activation during OC. In vitro, isolated ECs entered the cell cycle but the cycle stabilized when they reached confluence.

### Cell cycle signaling in endothelial cells

**In vivo (reference).** Transcripts present and those absent in the reference group are represented in Figure 4 and detailed in Table S2 in File S1. The profile was compatible with early G1 phase arrest. For early G1 phase, CCND2 (Cyclin D2), CCND3 (Cyclin D3), CDK4 were present but not CDK6. For late G1 phase, CDK2 was present but not CCNE1 (Cyclin E1) or CCNE2 (Cyclin E2) transcripts, preventing CyclinE/CDK2 complexes from forming and entering the S phase. The presence of two CDK inhibitors CDKN1A (p21<sup>CIP1</sup>) and CDKN1B (p27<sup>KIP1</sup>) suggested inhibition of CDK2 and CDK4, preventing formation of CyclinE/CDK2 and CyclinD/CDK4 complexes. For progression from G1 to the S phase, RBL1 transcript was present but not E2F transcription factors (except for E2F5), *CDC7* (G1/S), *CDC45* (S) or MKI67 (Ki67). The CDC25A transcript required for activation of CDKs was also absent. Markers of G2 and S phase entry were absent: CCNA1 (Cyclin A1), CCNA2 (Cyclin A2), CCNB1 (Cyclin B1), CCNB2 (Cyclin B2). For the G2 to M phase, the presence of ATR and ATM transcripts suggested the activation of DNA damage checkpoints. The presence of NBN (Nibrin), GADD45A and CDKN1A (p21<sup>CIP1</sup>) transcripts may result in CDK2 inactivation and cell cycle arrest. The absence of M phase transcripts, such as MCM complexes (except for MCM2), confirmed the absence of cell division. Several transcripts whose proteins are involved in the large ubiquitin-mediated degradation complex were expressed: three anaphase-promoting complex (APC) subunits, three culins, and *CDC16*. Notably, no transcript

of Cyclin D1, or p53 or p16<sup>Ink4A</sup>, was found. The five other EC types were compared to this baseline expression profile.

### Functional analysis (Fig. 5)

**Expression of cyclins and cyclin-dependent kinases.** For G1 to S phase, in tissue models, only cyclin D2 was overexpressed in OC. Cyclin D1 and D3 showed no significant change in any conditions. Cyclin D1, not detected in vivo, was increasingly expressed in CPC, NCPC and the ECL. Similarly, cyclin E1 and E2, not detected in vivo, were expressed in OC and primary cultures. For the formation of cyclin/CDK complexes, the level of CDK4 expression detected in vivo did not change significantly in any conditions. Only CDK6 expression, not detected in vivo, was present in the ECL. These observations suggest that the lack of expression of cyclin D1, E1, E2 and CDK6 may be responsible for EC cell-cycle arrest in G1 phase. S to G2 and M phase cyclins (A1, A2, B1, B2) and CDC2 not detected in vivo were expressed only in NCPC and the ECL. These findings were consistent with proliferation observed in both cell types. CDK2 level increased slightly only in OC and the ECL.

**Cyclin-dependent kinase inhibitors.** Notably, CDKN1A (p21) expression was unchanged in all conditions. CDKN2A (p16) was overexpressed in the three in vitro cell culture models. CDKN2B (p15), CDKN2C (p18), and CDKN2D (p19) were overexpressed in OC and also in vitro. CDKN3 significantly increased only in the three in vitro cell culture models.

### Analysis by biological model (Fig. 6)

**Post-mortem group.** The total quantity of over/under-represented transcripts was lower than in other groups. The pair-wise comparison of RNA normalized expression values between in vivo and post-mortem identified 59/112 transcripts with  $\geq 1.5$ -fold changes in expression (48 overexpressed, 11 underexpressed). The most over-represented transcripts were *CKS2* (+4.3 fold), *TP53* (p53) (+3.6 fold), *MAD2L2* (+3.4 fold), *CCNC* (+3.3 fold) (Table 4). Over-represented transcripts mainly comprised genes potentially associated with cell cycle arrest: *TP53* and *GADD45A*, both cyclin G, which are associated with DNA-

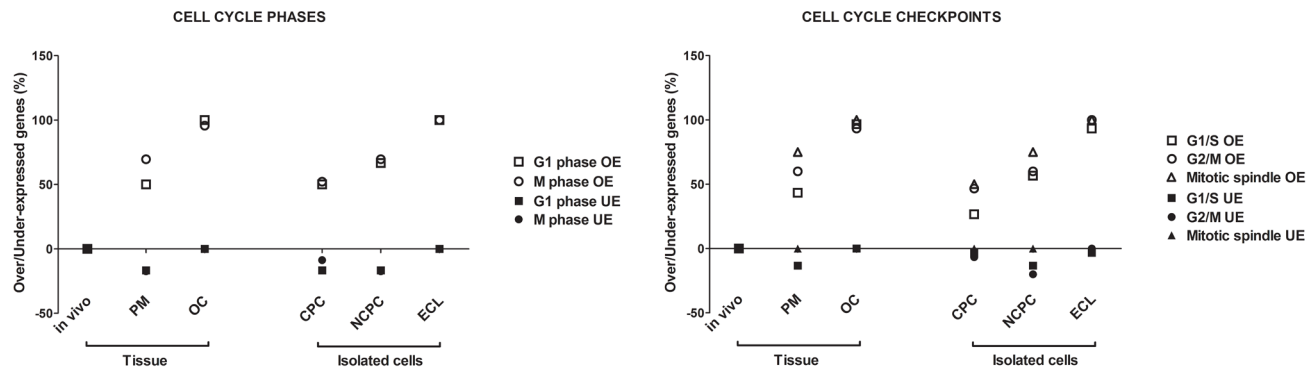


**Figure 3. Variations of genes implicated in cell cycle phases and checkpoints.** Percentage of genes overexpressed (OE) or underexpressed (UE) compared to in vivo condition (fold-change  $\geq 1.5$ ) in ECs of the different biological models: post mortem (PM), organ culture (OC), confluent primary culture (CPC), non-confluent primary culture (NCPC), and endothelial cell line (ECL). S and G2-phase genes (n = 4, see Table S1 in File S1), were not shown.  
doi:10.1371/journal.pone.0094349.g003



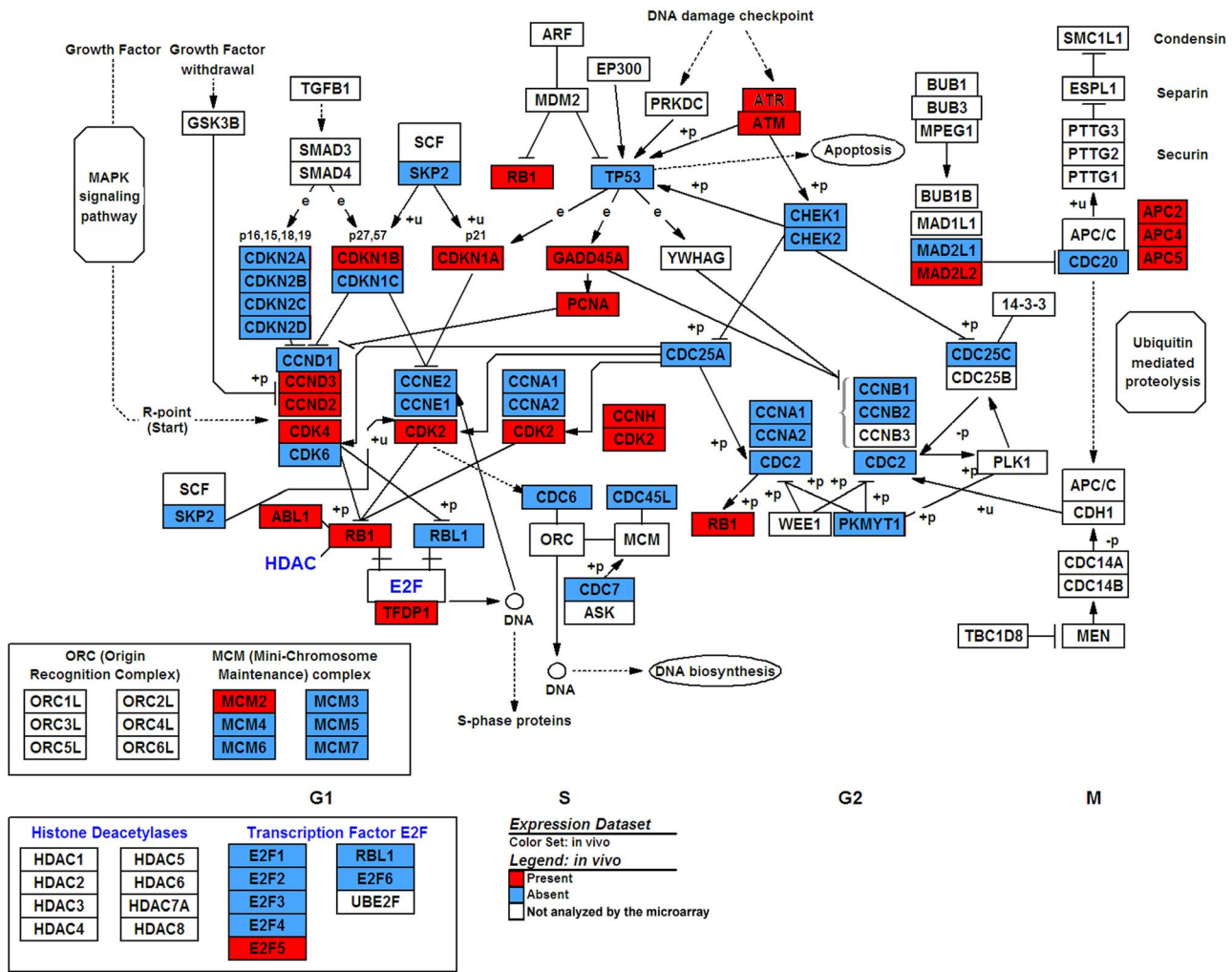


**Figure 4. Baseline cell cycle gene expression profile in human corneal endothelial cells in vivo.** Graphic representation of the presence/absence of gene expression on KEGG cell cycle pathway using GenMAPP version 2.1 (<http://www.genmapp.org/>). doi:10.1371/journal.pone.0094349.g004

induced damage (Cyclin G1 is associated with the p53 pathway [52]; cyclin G2 inhibits proliferation in models of ovarian [53] or gastric [54] cancers); cyclin C, which is a candidate tumor suppressor gene in osteosarcoma [55] and actively maintains quiescence in hematopoietic stem/progenitor cells [56]; *MAD2-1* and *MAD2-2*, two of the essential mitotic spindle checkpoint regulators, which have been associated with limitation of proliferation in a gastric-cancer model [57]; and p57Kip2, a strong inhibitor of several G1 phase cyclin/Cdk complexes and a negative regulator of cell proliferation [58]. In contrast, only three transcripts of pro-proliferative genes were found to be over-represented: *CKS2*, essential for cell cycle progression and associated with proliferation in gastric cancer [59]; *CDK7*, which functions as a CDK-activating kinase (CAK) and has also been identified as an essential component of the transcription factor TFIIH, which is involved in transcription initiation and DNA repair [60,61,62]; and *MCM7*, critical for cell proliferation and maintaining genome stability [63]. Other genes were absent or under-represented.

**Organ culture group.** The pair-wise comparison of RNA normalized expression values between in vivo and OC identified 58/112 transcripts with >1.5-fold changes in expression (all

overexpressed). Among the transcripts with the largest fold change in expression (Table 4), the most interesting observation was that several over-represented transcripts, not previously reported, encoded proteins implicated in cell cycle arrest. The most over-represented transcripts were *DIRAS3*(*ARH1*) (+32.1 fold), *CCNF* (cyclin F) (+13.1 fold), *CDKN2D* (p19<sup>Ink4d</sup>), (+13.1 fold), *CDKN2B* (p15<sup>Ink4b</sup>) (+11.8 fold). Notably, multiple transcripts of proteins implied in cell cycle arrest in response to DNA damage were over-represented. Several other transcripts encoding pro-proliferative proteins were over-represented: *CCNE1*, *CCNE2*, *CCND2*, *CDK2*, *CDK4*, *E2F2*.

**Confluent primary culture.** The pair-wise comparison of RNA normalized expression values between in vivo and confluent primary cultures identified 32 transcripts with ≥1.5 fold changes in expression (23 overexpressed, 9 underexpressed). Among the transcripts with the largest fold changes in expression (Table 4) were six of the top 10 encoded proteins implicated in cell cycle arrest (DNA-damaged induced or CKI) and four of the top 10 encoded proteins implicated in proliferation and cell survival. The four most over-represented transcripts were *DIRAS3* (+43.1 fold), *BIRC5* (Survivin) (+38.9 fold), *CCNB1* (cyclin B1)(+24.3 fold), and *CDKN2B* (p15<sup>Ink4b</sup>) (+11.8 fold). The most under-represented

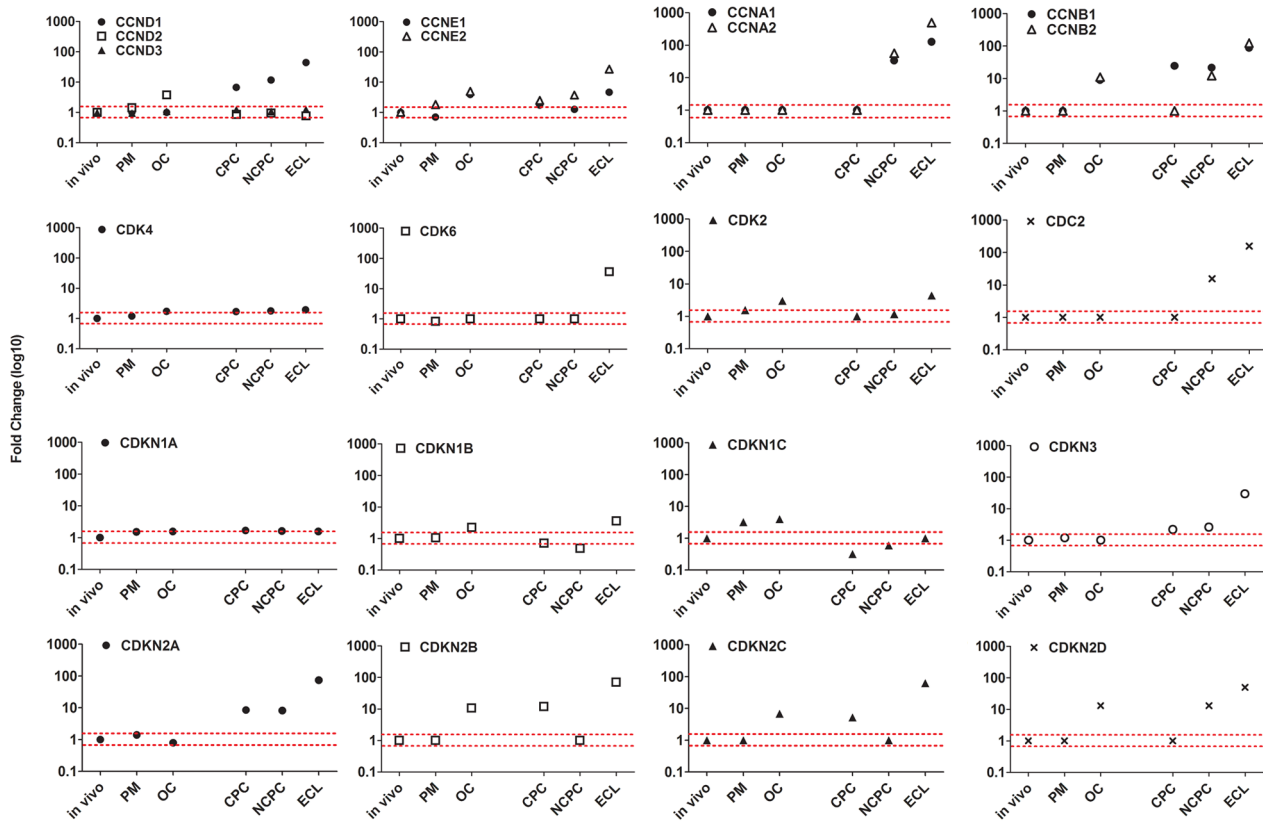


**Figure 5. Analysis of mRNA expression of cyclins, CDKs and CKIs in endothelial cells exposed to 6 different environments.** Fold-change expressions of in vivo (reference), post mortem (PM), organ culture (OC), confluent primary culture (CPC), non-confluent primary culture (NCP), and endothelial cell line (ECL) models were represented in logarithmic scale. The red dotted lines show limits of under/overexpression (fold-change  $\geq 1.5$ ).

doi:10.1371/journal.pone.0094349.g005

transcripts were *UBE1* (-3.3 fold), *ANAPC5* (-2.5 fold), *TFDP1* (-2.0 fold), *E2F5* (-1.9 fold). Confluent primary culture also exhibited overexpression of transcripts of the proliferation marker *Ki67*, underexpression of *CDKN1B* (p27<sup>KIP1</sup>) but overexpression of three other CKIs (*CDKN2B* (p15<sup>Ink4b</sup>), *CDKN2A* (p16<sup>Ink4a</sup>), *CDKN2C* (p18<sup>Ink4c</sup>)), the associated cdk2 inhibitor transcript *CDKN3*, and p21<sup>CIP1</sup> associated transcript *BCCIP*.

**Non-confluent primary culture.** Confluent and non-confluent primary cultures exhibited similar profiles. The pair-wise comparison of RNA normalized expression values between in vivo and confluent primary cultures identified 36 transcripts with  $\geq 1.5$  fold changes in expression (22 overexpressed, 14 underexpressed). Among the transcripts with the largest change in expression (Table 4) were three of the top 10 encoded proteins implicated in cell cycle progression and four encoded proteins implicated in cell cycle inhibition. The four most overrepresented transcripts were *BIRC5* (survivin) (+50.9 fold), *CCNB1* (cyclin B1) (+21.7 fold), *BRCA2* (+15.0 fold), and *CDC20* (+14.5 fold). The most underrepresented transcripts were *CUL5* (-8.8 fold), *RBI* (-4.1 fold), *CDK5R2* (-3.3 fold), and *DDX11* (-2.9 fold). Transcripts of proliferation markers (*Ki67* and *MCM2*) were overrepresented. Non-confluent culture overexpressed fewer CKIs than confluent culture.

**Cell line.** The proliferative cell line exhibited a completely different transcriptional profile. The pair-wise comparison of RNA normalized expression values between in vivo and cell line identified 85 transcripts with  $\geq 1.5$  fold changes in expression (all overexpressed). Among the transcripts with the largest fold change

in expression (Table 4), the most interesting observation was that several transcripts overrepresented in the cell line encoded proteins implicated in cell proliferation. The most overrepresented transcripts were *CCNA2* (+492.1 fold), *CDC2* (+156.8 fold), *CDC6* (+135.3 fold), *CCNB2* (+123.4 fold). The cell line exhibited expression changes in several groups of genes; and interestingly, numerous transcripts of cell cycle negative regulators were overrepresented too. Note that *DIRAS3*, overrepresented in OC and in both in vitro cultures, was not found in the ECL.

### Real-time PCR confirmation of microarrays

A subset of 11 transcripts, over- or under-represented in microarrays depending on EC type, was tested using qRT-PCR. Differential gene expression was consistent between the two independent methods of analysis, and the level of expression of the 11 genes changed in the same direction, although there were quantitative differences between the results of gene array analysis and of quantitative real-time PCR (Fig. 7). Spearman's correlation coefficient ( $\rho$ ) between microarray and qRT-PCR results was 0.8218 ( $p < 0.001$ ), confirming a very high level of agreement.

### Discussion

In the present study, gene array technology was used to examine differential cell cycle gene expression in human corneal ECs that exhibit different proliferation status. A focused cDNA array was chosen. We identified several differentially expressed genes, especially those implicated in G1-phase arrest and in DNA

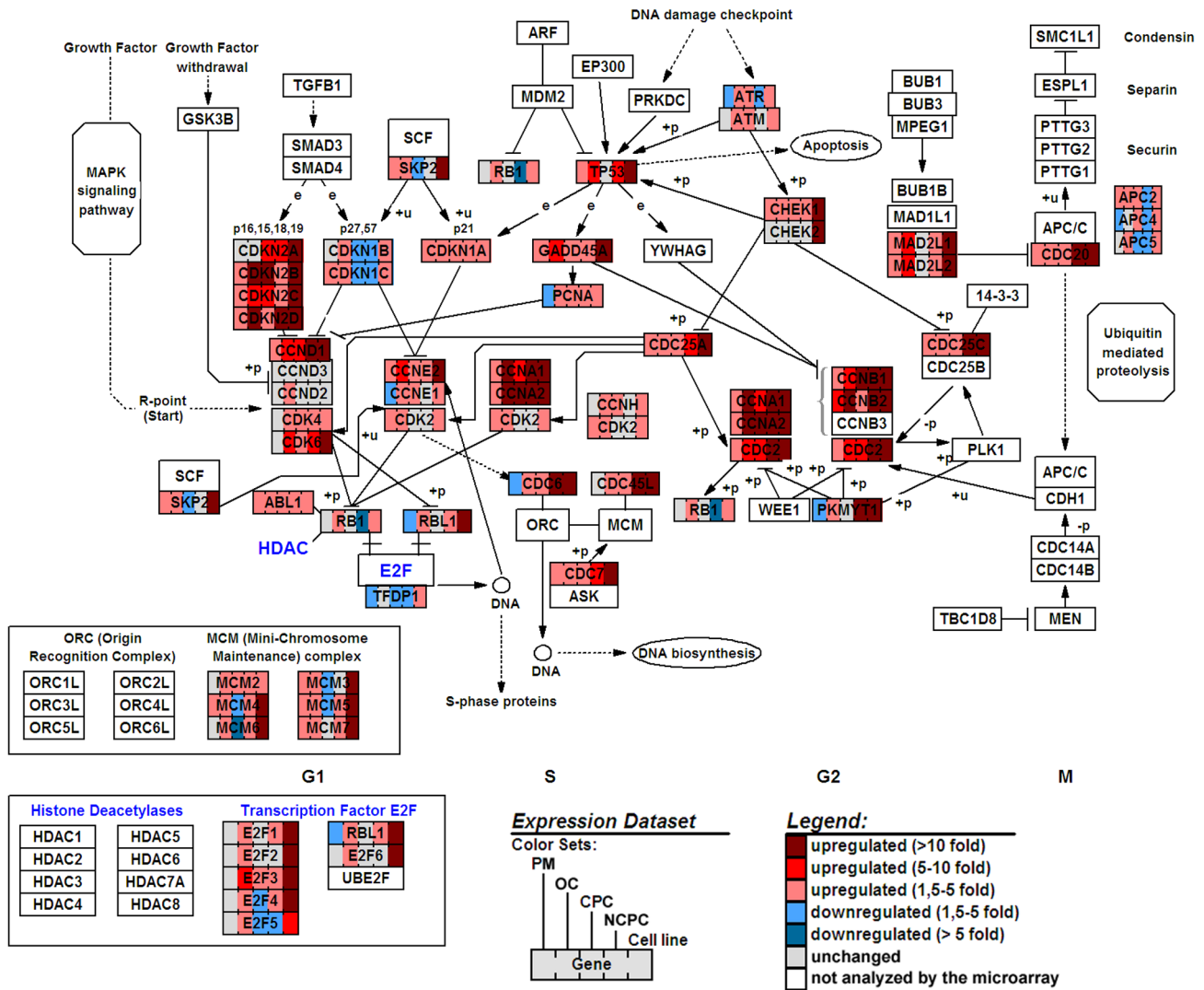


**Figure 6. Gene map of cell cycle genes differentially expressed by human corneal endothelial cells in six biological models.** Post mortem (PM), corneal organ culture (OC), in vitro confluent primary culture (CPC), in vitro non-confluent primary culture (NCPC), and immortalized endothelial cell line (ECL). Results were compared with in vivo endothelial cells. The representation of the pathway was generated by GenMAPP version 2.1 (<http://www.genmapp.org/>) using the cell cycle pathway provided by KEGG. doi:10.1371/journal.pone.0094349.g006

damage-induced cell cycle arrest in other cell types. While it is beyond the scope of this report to highlight the potential significance of each altered gene, some are of unique interest and warrant specific mention. Although less sensitive than SAGE, SADE or the most recent RNA-sequencing techniques, microarrays enable focused assessment of gene expression in a given tissue. In Gottsh, 10% of SAGE tags were devoted to cell growth and regulation, so it was likely that specific arrays could identify specific variations in cell cycle-related transcripts in ECs. Focused analysis and transcript classification confirmed the logical evolution of the profiles from in vivo to ECL, or from the least to the most proliferative status.

**Study limitations**

Despite a high level of agreement between qRT-PCR and microarrays, the changes in expression detected by microarray analysis were generally smaller than those derived by qRT-PCR as previously described [37]. This may be due to the different detection ranges of these two techniques. It has been demonstrated

that microarrays tend to have a low dynamic range, which could lead to under-representation of changes in gene expression, whereas qRT-PCR has a high dynamic range [64]. This may also explain why *CCND1*, *CDKN1A*, and *MKI67*, or changes thereto, were not detected by microarray in certain groups but were detected by real-time PCR.

Ages in the in vivo group were lower than in the other groups because keratoconus patients are younger than corneal donors. In most European countries and particularly in France, where no upper age limit exists for corneal donation, mean donor age is 72 years [14]. The corneas studied in this paper are thus close in age to those routinely grafted, making it difficult to distinguish differences in transcription levels due respectively to donor aging and to environment (post-mortem stress, OC, in vitro cell culture). Donor age was significantly higher than in other studies, and our results are consequently difficult to compare, since a systemic decrease in transcription and translation with age has been described [65].

**Table 4.** Top gene expression changes.

|                      | OVEREXPRESSION |   |   | UNDEREXPRESSION |   |   |       |
|----------------------|----------------|---|---|-----------------|---|---|-------|
|                      | Gene symbol    | Gene title  | Fold change   | Gene symbol     | Gene title  | Fold change   |       |
| <b>Post - mortem</b> | CKS2           | CDC28 protein kinase regulatory subunit 2   | 4.27  | ATR             | Ataxia telangiectasia and Rad3 related  | -2.47   |       |
|                      | TP53           | Tumor protein p53 (Li-Fraumeni syndrome)  | 3.56  | BAX             | BCL2-associated X protein   | -2.10   |       |
|                      | MAD2L2         | MAD2 mitotic arrest deficient-like 2 (yeast)  | 3.39  | CUL4A           | Cullin 4A   | -2.08   |       |
|                      | CCNC           | Cyclin C  | 3.35  | CDK5R2          | Cyclin-dependent kinase 5, regulatory subunit 2 (p39)   | -2.05   |       |
|                      | SERTAD1        | SERTA domain containing 1   | 3.26  | ANAPC4          | Anaphase promoting complex subunit 4  | -1.98   |       |
|                      | CDKN1C         | Cyclin-dependent kinase inhibitor 1C (p57, Kip2)  | 3.22  | TFDP1           | Transcription factor Dp-1   | -1.80   |       |
|                      | CCNG2          | Cyclin G2   | 3.00  | KPNA2           | Karyopherin alpha 2 (RAG cohort 1, importin alpha 1)  | -1.74   |       |
|                      | MCM7           | MCM7 minichromosome maintenance deficient 7 ( <i>S. cerevisiae</i> )                    | 2.64  | PCNA            | Proliferating cell nuclear antigen  | -1.54   |       |
|                      | MAD2L1         | MAD2 mitotic arrest deficient-like 1 (yeast)  | 2.25  |                 |   |   |       |
|                      | CCNG1          | Cyclin G1   | 2.15  |                 |   |   |       |
|                      | CDK7           | Cyclin-dependent kinase 7 (MO15 homolog, <i>Xenopus laevis</i> , cdk-activating kinase) | 1.99  |                 |   |   |       |
|                      | <b>OC</b>      | DIRAS3  | DEAD/H (Asp-Glu-Ala-Asp/His) box polypeptide 11 (CHL1-like helicase homolog, <i>S. cerevisiae</i> ) | 32.08           |   |   |       |
|                      |                | CCNF  | Cyclin F  | 13.14           |   |   |       |
|                      |                | CDKN2D  | Cyclin-dependent kinase inhibitor 2D (p19, inhibits CDK4)   | 13.05           |   |   |       |
| CCNB2                |                | Cyclin B2   | 10.95   |                 |   |   |       |
| CDKN2B               |                | Cyclin-dependent kinase inhibitor 2B (p15, inhibits CDK4)                               | 10.52   |                 |   |   |       |
| CCNC                 |                | Cyclin C  | 9.88  |                 |   |   |       |
| CCNB1                |                | Cyclin B1   | 8.97  |                 |   |   |       |
| GADD45A              |                | Growth arrest and DNA-damage-inducible, alpha   | 7.96  |                 |   |   |       |
| CUL2                 |                | Cullin 2  | 7.84  |                 |   |   |       |
| CCNT2                |                | Cyclin T2   | 7.71  |                 |   |   |       |
| CDK5RAP3             |                | CDK5 regulatory subunit associated protein 3  | 7.35  |                 |   |   |       |
| CDK7                 |                | Cyclin-dependent kinase 7 (MO15 homolog, <i>Xenopus laevis</i> , cdk-activating kinase) | 7.27  |                 |   |   |       |
| CCNG2                |                | Cyclin G2   | 6.78  |                 |   |   |       |
| <b>CPC</b>           |                | DIRAS3  | DEAD/H (Asp-Glu-Ala-Asp/His) box polypeptide 11 (CHL1-like helicase homolog, <i>S. cerevisiae</i> ) | 43.06           | UBE1  | Ubiquitin-activating enzyme E1 (A1S9T and BN75 temperature sensitivity complementing) | -3.33 |
|                      | BIRC5          | Baculoviral IAP repeat-containing 5 (survivin)  | 38.92   | ANAPC5          | Anaphase promoting complex subunit 5  | -2.49   |       |
|                      | CCNB1          | Cyclin B1   | 24.30   | TFDP1           | Transcription factor Dp-1   | -2.01   |       |
|                      | CDKN2B         | Cyclin-dependent kinase inhibitor 2B (p15, inhibits CDK4)                               | 11.83   | CCNG1           | Cyclin G1   | -1.62   |       |
|                      | CKS2           | CDC28 protein kinase regulatory subunit 2   | 9.64  | DDX11           | DEAD/H (Asp-Glu-Ala-Asp/His) box polypeptide 11 (CHL1-like helicase homolog, <i>S. cerevisiae</i> ) | -1.56   |       |

**Table 4.** Cont.

| OVEREXPRESSION |   |             | UNDEREXPRESSION |  |             |
|----------------|---|-------------|-----------------|--|-------------|
| Gene symbol    | Gene title  | Fold change | Gene symbol     | Gene title                                       | Fold change |
| CDKN2A         | Cyclin-dependent kinase inhibitor 2A (melanoma, p16, inhibits CDK4)                                 | 8.51        |                 |  |             |
| CCND1          | Cyclin D1   | 6.66        |                 |  |             |
| CCNG2          | Cyclin G2   | 6.44        |                 |  |             |
| CDKN2C         | Cyclin-dependent kinase inhibitor 2C (p18, inhibits CDK4)   | 5.19        |                 |  |             |
| GADD45A        | Growth arrest and DNA-damage-inducible, alpha   | 4.51        |                 |  |             |
| <b>NCPC</b>    |   |             |                 |  |             |
| CCNA2          | Cyclin A2   | 56.21       | RB1             | Retinoblastoma 1 (including osteosarcoma)        | -4.06       |
| BIRC5          | Baculoviral IAP repeat-containing 5 (survivin)  | 50.85       | ANAPC2          | Anaphase promoting complex subunit 2             | -2.78       |
| CCNA1          | Cyclin A1   | 33.75       | CDKN1B          | Cyclin-dependent kinase inhibitor 1B (p27, Kip1) | -2.03       |
| CCNB1          | Cyclin B1   | 21.65       | ATR             | Ataxia telangiectasia and Rad3 related           | -1.99       |
| CDC2           | Cell division cycle 2, G1 to S and G2 to M  | 15.54       | ANAPC4          | Anaphase promoting complex subunit 4             | -1.81       |
| BRCA2          | Breast cancer 2, early onset  | 14.96       | TFDP1           | Transcription factor Dp-1                        | -1.80       |
| CDC20          | Cell division cycle 20 homolog ( <i>S. cerevisiae</i> )   | 14.53       | CUL4A           | Cullin 4A  | -1.62       |
| CDC37          | Cell division cycle 37 homolog ( <i>S. cerevisiae</i> )   | 13.89       | ANAPC5          | Anaphase promoting complex subunit 5             | -1.51       |
| CDKN2D         | Cyclin-dependent kinase inhibitor 2D (p19, inhibits CDK4)   | 13.10       |                 |  |             |
| DIRAS3         | DEAD/H (Asp-Glu-Ala-Asp/His) box polypeptide 11 (CHL1-like helicase homolog, <i>S. cerevisiae</i> ) | 12.81       |                 |  |             |
| <b>ECL</b>     |   |             |                 |  |             |
| CCNA2          | Cyclin A2   | 492.07      |                 |  |             |
| CDC2           | Cell division cycle 2, G1 to S and G2 to M  | 156.81      |                 |  |             |
| CDC6           | Cell division cycle 6 homolog ( <i>S. cerevisiae</i> )  | 135.25      |                 |  |             |
| CCNA1          | Cyclin A1   | 127.09      |                 |  |             |
| CCNB2          | Cyclin B2   | 123.42      |                 |  |             |
| BIRC5          | Baculoviral IAP repeat-containing 5 (survivin)  | 99.46       |                 |  |             |
| CCNB1          | Cyclin B1   | 87.46       |                 |  |             |
| CDC25C         | Cell division cycle 25 homolog C ( <i>S. pombe</i> )  | 76.85       |                 |  |             |
| CDKN2A         | Cyclin-dependent kinase inhibitor 2A (melanoma, p16, inhibits CDK4)                                 | 73.44       |                 |  |             |
| PKMYT1         | Protein kinase, membrane associated tyrosine/threonine 1  | 70.07       |                 |  |             |

doi:10.1371/journal.pone.0094349.t004

The *in vivo* group comprised only central ECs, whereas the other groups involved the whole endothelium, in which substantial differences in proliferative capacity between center and periphery were demonstrated [22,23]. This likely explains the specific profile found in the *in vivo* group, where most transcripts were associated with cell cycle arrest and more specifically growth arrest following DNA damage; and the presence in the other groups of both cell cycle arrest and pro-proliferative signatures, because neither central nor peripheral cells were separated.

Confluent and non-confluent primary cultures were grown from independent donors.

Microarrays are limited by the finite number of oligonucleotide sequences on a chip, and are not able to identify the expression of novel genes, contrary to SAGE or genome-wide assays. Nevertheless the 112 genes contained in the present chip covered all the cell cycle genes already described and numerous others never previously studied.

Protein expression remains to be demonstrated and quantified on selected candidates to validate microarrays and qRT-PCR

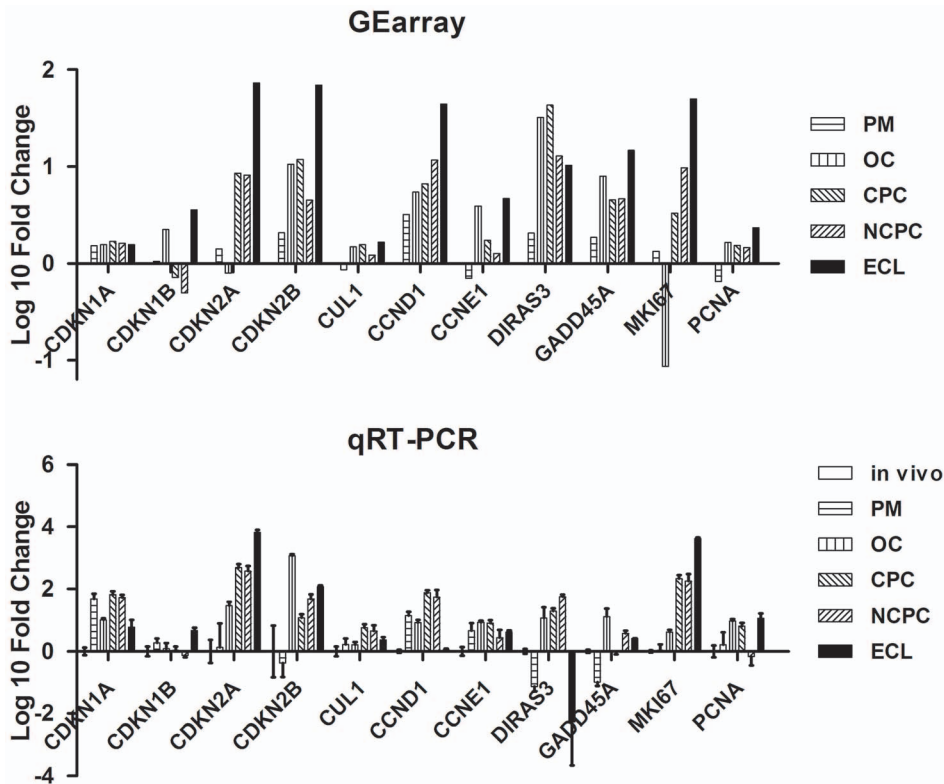


**Figure 7. Differentially expressed genes by endothelial cells of the six different biological models, confirmed by real-time PCR.** RNA (300 ng) was characterized using qRT-PCR profiling kit on a subset of 11 genes. Corresponding microarray results are shown. doi:10.1371/journal.pone.0094349.g007

findings, given that post-transcriptional modifications are very likely to occur, increasing the complexity of cell cycle controls. This will be our next step, using immunolabeling that we recently optimized for en face observation of intact ECs on flat mounted corneas [66].

#### Baseline transcription profile in vivo

For the first time, the cell cycle-related transcription profile of human ECs very close to in vivo physiological condition has been described using normal ECs collected immediately after explantation during a corneal graft. This profile is consistent with the previously known proliferative status determined using study of proteins involved in cell cycle regulation performed with donor corneas stored for 24–36 hours at 4°C [67], but provides much complementary information. We found multiple transcripts compatible with early G1 phase arrest of the cell cycle. *GADD45A*, *Nibrin (NBN or NBS1)*, *ATM* and *ATR*, four transcripts associated with DNA damage-induced cell cycle arrest, have been identified. These results are consistent with the recent findings of Joyce et al. [68] using PCR-based microarray (and Western blots for *GADD45A* and *ATM*) and with the previously described nuclear oxidative DNA damage in ECs of donors aged over 50 years, with a predominance of lesions in the central corneal area [65]. These lesions are likely induced by cumulative low-dose exposure to UV radiation throughout life (the major part of UV wavelengths being attenuated by the epithelial and stromal layers) and may be modulated by frequent temperature variations of the cornea. At chromosome level, an age-related accumulation of errors was described in human ECs, with an age-related increase in the relative number of polyploid cells with >4N DNA content and cells with multiple nuclei in otherwise healthy human corneal

endothelium [69,70]. Similar increases in DNA content were observed in adult endothelium in response to injury [71].

Several actors in the ubiquitin/proteasome complex implicated in the regulation of CDK/Cyclin and CKI have also been found, confirming that ECs actively regulate their non-proliferative profile and are not excluded from the cell cycle. Our results differ slightly from the literature regarding three transcripts: *CCND1*, *TP53* and *CDN2A*. We found no expression of *CCND1* or *CDKN2A* in microarrays, only in qRT PCR (see above for technical discussion). Until now, the three cyclin-D isoforms had not been studied separately in human ECs [67,72]. The *CCND1* protein (cyclin D1) had been described only in in vitro rat corneal endothelial cells [73]. Cyclin D isoform may have redundant functions and is not distributed equally in all tissues [74]. Nevertheless, the absence of cyclin D1 may be associated with the non-proliferative status of ECs in vivo, as overexpression was observed in OC and in the three types of cell culture. Notably, it has recently been demonstrated that the forced overexpression of *CDK4/Cyclin D1* in human ECs led to the establishment of functioning ECL with high growth potential [75]. *CDKN2A* (p16<sup>Ink4a</sup>) was not found either, although expression of the corresponding protein in EC nuclei has already been described, with expression increasing with donor age [24,72,76]. This difference is unlikely explained by the donor age in our experiments because *CDKN2A* was not more strongly expressed in the OC group, although donors were older than in the in vivo group. The difference in tissue origin and storage method may be partly responsible, p16<sup>Ink4a</sup> having been described in post-mortem cornea with short-term cold storage [24,72,76]. Conversely we found *CDKN2A* in cell cultures, as already described [24]. *TP53* transcript was not found either in microarrays (not tested with

qRT-PCR), although the protein has previously been described in human donor cornea after short-term cold storage [72,77,78]. The difference could be explained by the absence of post-mortem and storage-induced stress in our *in vivo* samples. Moreover, p53 transcript was one of the most overrepresented in the post-mortem group. Lastly, we found only one of the EF2 transcription factors, E2F5, whose particular role in the early G1 phase has already been described [79].

### Donor cornea

High post-mortem stress is liable to induce profound changes in gene transcription. Unsurprisingly, the level of change in our study remained low, indicating a global decrease in cell metabolism. Nevertheless, the well-known long survival of corneal EC after donor death (successful grafts with corneas retrieved up to 72 hours post death are regularly observed, and longer post-mortem times have also been described more anecdotally) explains the possibility of observing significant transcriptional changes. DNA damage appears to activate cell cycle arrest mechanisms through overexpression of several genes involved in the p53-dependent or -independent pathways. Interestingly, *culin4A*, implicated in the limitation of DNA-damage repair capacity in UV-induced skin cancers [80], is under-represented in this group, and this may correspond to a response adopted to increase cellular DNA repair capacity.

### Organ-cultured corneas

Genomic study of OC corneas is also original because only corneas stored at 4°C had previously been studied. Routine OC with conventional medium (MEM+2% FCS) is the main method used for cornea storage in Europe. By promoting cell metabolism in cell culture-derived medium at 31–34°C (as per eye bank protocol) it allows storage for up to 5 weeks, unlike the current 5–6 days allowed by the cold storage at 4°C common in the USA. OC is not known to promote EC proliferation, although it facilitates endothelial wound healing by migration of cells in the vicinity of the local defect in the endothelial layer [13]. Only OC with 8% FCS, a method that remains an exception [14], seems likely to promote cell mitosis [15]. It was thus important to determine whether routine OC induces significant transcriptional profile changes liable to reveal the stimulation of certain ECs with residual proliferative capacity. In our samples, the majority of the transcripts are associated with cell cycle arrest mechanisms, but several others were implicated in G1/S transition, suggesting that ECs did not behave homogeneously in OC. The percentage of cells progressing in the cell cycle remains to be determined, but similar focused microarrays were sensitive enough to detect as little as 10% contamination from a specific cell subpopulation [81].

Up to now, the role of three CKIs (p21<sup>Cip1</sup>, p27<sup>Kip1</sup>, and p16<sup>Ink4a</sup>) has been demonstrated. We have highlighted the probable role of the third CIP/KIP p57<sup>Kip2</sup> and the three other INK4 family members p15<sup>Ink4b</sup>, p18<sup>Ink4c</sup>, p19<sup>Ink4d</sup>, whose transcripts were found to be overexpressed. The absence of p16<sup>Ink4a</sup> transcript has been discussed above. Our results suggest that cell cycle inhibition is redundantly controlled in OC. Interestingly, other transcripts associated with cell cycle arrest were over-represented, especially *DIRAS3* (also over-represented in primary cell cultures but absent in the ECL). *DIRAS3*, also known as A ras homologue member 1 (*ARHI*) is a maternally imprinted human tumor suppressor gene that encodes a small G protein with 50–60% aminoacide homology to Rap and Ras. It has been extensively studied in various cancer types. In ovarian and breast cancer, reexpression of *ARHI* inhibits cancer cell growth *in vitro* and *in vivo*, induces p21<sup>WAF1</sup> and downregulates

cyclin D1 promoter activity [82]. In pancreatic cancer, *ARHI* blocks cell progression in cell cycle phase G1, and increases p21<sup>Cip1</sup> through the accumulation of p53 protein. *ARHI* enhances expression of p27<sup>Kip1</sup> through inhibition of PI-3K/AKT signaling [83]. Note that the Pi-3K/AKT signaling pathway has been described in rabbit ECs in response to FGF-2 stimulation *in vitro* [84]. However, *DIRAS3* was not found in the CorneaNet database nor in the recent study by Joyce et al [68]. Besides *DIRAS3*, several transcripts whose proteins are involved in cell cycle arrest and DNA damage repair in response to DNA damage were described in OC: *GADD45A*, *NBN*, *ATM* and *ATR* already present in the *in vivo* group, associated with *RAD1*, *RAD9A*, *TP53*, *BCRA1*, and *CCNG1*.

The role of *CUL4* should also be further investigated because of its particular relevance in controlling DNA repair capacities. We found its transcript in *in vivo* EC, underexpressed in the primary cultures, and over-represented in OC and the ECL. The *CUL4A-E3* ligase is involved in the ubiquitination of various protein substrates around the site of UV-induced DNA damage [85]. It is associated with UV-damaged DNA-binding protein 2 that has been described as highly expressed in human EC [86]. By analogy with descriptions made in UV-induced skin carcinogenesis in mice, in which *CUL4* ubiquitin ligase restricts cellular repair capacity [80], overexpression of *CUL4* in OC or the ECL may suggest that ECs do not operate at their full DNA repair potential, and highlight the potential increase in cell repair proficiency by pharmacological *CUL4A* inhibition.

### In vitro primary cell cultures

Confluent and non-confluent cultures did not differ fundamentally in profile. Like ECs from OC corneas, they exhibited cell cycle arrest-associated transcripts, be they CKIs, cell cycle checkpoints, or DNA damage-induced. Conversely, they also logically expressed transcripts associated with proliferation such as G1/S and G2/M cyclins, or proliferation markers. One of the most overexpressed transcripts was that of the anti-apoptotic protein survivin, which may be stimulated by cell culture-associated stress. Interestingly, the CKI p27<sup>KIP1</sup> was found to be under-represented, although it was associated with mitotic inhibition induced by cell-cell contact in neonatal rat ECs [87,88]. This result suggests that contact inhibition in confluent culture may be less efficient than *in vivo*, and/or that the mechanism in humans may involve other CKIs than only p27<sup>KIP1</sup>.

### Cell line

The SV40LT transformed ECL overexpressed almost all cell cycle-related genes in the microarray. The most up-regulated genes were logically associated with cell cycle progression and were consistent with the mechanisms of SV40LT transformation [89]: CDK/cyclin of the G1/S and G2/M transitions, E2F transcription factors, proliferation markers and MCM replication complex, with *CCNA2* and *CDC2* (both G2/M) being the two most over-represented. Conversely, cycle inhibitors (CKIs, checkpoints, DNA damage-induced inhibitors) were also strongly over-represented. A first hypothesis for the double profile relies on good contact inhibition of the cell line that, despite high proliferative capacity, strictly grows in a monolayer until it reaches very high cell density. A second explanation could be the existence of a double population in the cell line, with opposite differentiation and proliferation profiles [16,19]. High expression of anti-apoptotic proteins is common in immortalized cells, especially IAPs [90]. Notably, the absence of overexpression of *DIRAS3* in those proliferative cells suggests it plays a role in mitosis inhibition in non-transformed ECs, where it is always present.

In conclusion, cell cycle-specific cDNA arrays identified several candidate genes that may actively repress EC proliferation in humans and thus help us understand the premature senescence in human ECs previously described [8,23,91]. These genes are thus a useful resource for further mechanistic studies. Several of them could be targets for triggering and controlling cell proliferation, with a view to developing a cell therapy for corneal endothelial dystrophies.

## Supporting Information

**File S1 Supporting tables. Table S1.** Functional classification by cell cycle phase (using DAVID version 6.7, 2013 (<http://david.abcc.ncifcrf.gov/>)) of the 62/112 transcripts obtained with the Oligo GEArray Human cell cycle Microarray. 40/112

## References

1. Stocker FW (1953) The endothelium of the cornea and its clinical implications. *Trans Am Ophthalmol Soc* 51: 669.
2. Maurice DM (1970) The transparency of the corneal stroma. *Vision Res* 10: 107–108.
3. Murphy C, Alvarado J, Juster R, Maglio M (1984) Prenatal and postnatal cellularity of the human corneal endothelium. A quantitative histologic study. *Invest Ophthalmol Vis Sci* 25: 312–322.
4. Ko MK, Park WK, Lee JH, Chi JG (2001) A histomorphometric study of corneal endothelial cells in normal human fetuses. *Exp Eye Res* 72: 403–409.
5. Bourne WM, Nelson LR, Hodge DO (1997) Central corneal endothelial cell changes over a ten-year period. *Invest Ophthalmol Vis Sci* 38: 779–782.
6. Joyce NC (2003) Proliferative capacity of the corneal endothelium. *Prog Retin Eye Res* 22: 359–389.
7. Joyce NC (2012) Proliferative capacity of corneal endothelial cells. *Exp Eye Res* 95: 16–23.
8. Sheerin AN, Smith SK, Jennert-Burston K, Brook AJ, Allen MC, et al. (2012) Characterization of cellular senescence mechanisms in human corneal endothelial cells. *Aging Cell* 11: 234–240.
9. Insler MS, Lopez JG (1991) Heterologous transplantation versus enhancement of human corneal endothelium. *Cornea* 10: 136–148.
10. Okumura N, Koizumi N, Ueno M, Sakamoto Y, Takahashi H, et al. (2012) ROCK inhibitor converts corneal endothelial cells into a phenotype capable of regenerating in vivo endothelial tissue. *Am J Pathol* 181: 268–277.
11. McGowan SL, Edelhauser HF, Pfister RR, Whikchart DR (2007) Stem cell markers in the human posterior limbus and corneal endothelium of unwounded and wounded corneas. *Mol Vis* 13: 1984–2000.
12. He Z, Campolmi N, Gain P, Minh Hathi B, Dumollard JM, et al. (2012) Revisited Microanatomy of the Corneal Endothelial Periphery: New Evidence for Continuous Centripetal Migration of Endothelial Cells in Humans. *Stem Cells* 30: 2523–2534.
13. Nejezpinska J, Juklova K, Jirsova K (2010) Organ culture, but not hypothermic storage, facilitates the repair of the corneal endothelium following mechanical damage. *Acta Ophthalmol* 88: 413–419.
14. European Eye Bank Association Directory, eighteenth edition (2010) Amsterdam.
15. Slettedal JK, Lyberg T, Roger M, Beraki K, Ramstad H, et al. (2008) Regeneration with proliferation of the endothelium of cultured human donor corneas with extended postmortem time. *Cornea* 27: 212–219.
16. Valtink M, Gruschwitz R, Funk RH, Engelmann K (2008) Two clonal cell lines of immortalized human corneal endothelial cells show either differentiated or precursor cell characteristics. *Cells Tissues Organs* 187: 286–294.
17. Gottsch JD, Seitzman GD, Margulies EH, Bowers AL, Michels AJ, et al. (2003) Gene expression in donor corneal endothelium. *Arch Ophthalmol* 121: 252–258.
18. Gottsch JD, Bowers AL, Margulies EH, Seitzman GD, Kim SW, et al. (2003) Serial analysis of gene expression in the corneal endothelium of Fuchs' dystrophy. *Invest Ophthalmol Vis Sci* 44: 594–599.
19. Bednarsz J, Teifel M, Friedl P, Engelmann K (2000) Immortalization of human corneal endothelial cells using electroporation protocol optimized for human corneal endothelial and human retinal pigment epithelial cells. *Acta Ophthalmol Scand* 78: 130–136.
20. Chen KH, Azar D, Joyce NC (2001) Transplantation of adult human corneal endothelium ex vivo: a morphologic study. *Cornea* 20: 731–737.
21. Zhu C, Joyce NC (2004) Proliferative response of corneal endothelial cells from young and older donors. *Invest Ophthalmol Vis Sci* 45: 1743–1751.
22. Konomi K, Zhu C, Harris D, Joyce NC (2005) Comparison of the proliferative capacity of human corneal endothelial cells from the central and peripheral areas. *Invest Ophthalmol Vis Sci* 46: 4086–4091.
23. Mimura T, Joyce NC (2006) Replication competence and senescence in central and peripheral human corneal endothelium. *Invest Ophthalmol Vis Sci* 47: 1387–1396.
24. Enomoto K, Mimura T, Harris DL, Joyce NC (2006) Age differences in cyclin-dependent kinase inhibitor expression and rb hyperphosphorylation in human corneal endothelial cells. *Invest Ophthalmol Vis Sci* 47: 4330–4340.
25. Kikuchi M, Zhu C, Senoo T, Obara Y, Joyce NC (2006) p27kip1 siRNA induces proliferation in corneal endothelial cells from young but not older donors. *Invest Ophthalmol Vis Sci* 47: 4803–4809.
26. Mergler S, Dannowski H, Bednarsz J, Engelmann K, Hartmann C, et al. (2003) Calcium influx induced by activation of receptor tyrosine kinases in SV40-transfected human corneal endothelial cells. *Exp Eye Res* 77: 485–495.
27. Saghizadeh M, Kramerov AA, Tajbakhsh J, Aoki AM, Wang C, et al. (2005) Proteinase and growth factor alterations revealed by gene microarray analysis of human diabetic corneas. *Invest Ophthalmol Vis Sci* 46: 3604–3615.
28. Tanwar MK, Gilbert MR, Holland EC (2002) Gene expression microarray analysis reveals YKL-40 to be a potential serum marker for malignant character in human glioma. *Cancer Res* 62: 4364–4368.
29. Desai KV, Michalowska AM, Kondaiah P, Ward JM, Shih JH, et al. (2004) Gene expression profiling identifies a unique androgen-mediated inflammatory/immune signature and a PTEN (phosphatase and tensin homolog deleted on chromosome 10)-mediated apoptotic response specific to the rat ventral prostate. *Mol Endocrinol* 18: 2895–2907.
30. Bustin SA (2002) Quantification of mRNA using real-time reverse transcription PCR (RT-PCR): trends and problems. *J Mol Endocrinol* 29: 23–39.
31. Menendez L, Benigno BB, McDonald JF (2004) L1 and HERV-W retrotransposons are hypomethylated in human ovarian carcinomas. *Mol Cancer* 3: 12.
32. Lee PD, Sladek R, Greenwood CM, Hudson TJ (2002) Control genes and variability: absence of ubiquitous reference transcripts in diverse mammalian expression studies. *Genome Res* 12: 292–297.
33. Zweitig DR, Smirnov DA, Connelly MC, Terstappen LW, O'Hara SM, et al. (2007) Physiological stress induces the metastasis marker AGR2 in breast cancer cells. *Mol Cell Biochem* 306: 255–260.
34. Kosaka Y, Mimori K, Fukagawa T, Ishikawa K, Etoh T, et al. (2007) Identification of the high-risk group for metastasis of gastric cancer cases by vascular endothelial growth factor receptor-1 overexpression in peripheral blood. *Br J Cancer* 96: 1723–1728.
35. Veeriah S, Kautenburger T, Habermann N, Sauer J, Dietrich H, et al. (2006) Apple flavonoids inhibit growth of HT29 human colon cancer cells and modulate expression of genes involved in the biotransformation of xenobiotics. *Mol Carcinog* 45: 164–174.
36. DenBesten PK, Machule D, Zhang Y, Yan Q, Li W (2005) Characterization of human primary enamel organ epithelial cells in vitro. *Arch Oral Biol* 50: 689–694.
37. Bryan BA, Dyson OF, Akula SM (2006) Identifying cellular genes crucial for the reactivation of Kaposi's sarcoma-associated herpesvirus latency. *J Gen Virol* 87: 519–529.
38. Qu R, Li Y, Gao Q, Shen L, Zhang J, et al. (2007) Neurotrophic and growth factor gene expression profiling of mouse bone marrow stromal cells induced by ischemic brain extracts. *Neuropathology* 27: 355–363.
39. Kucukzeybek Y, Gul MK, Cengiz E, Erten C, Karaca B, et al. (2008) Enhancement of docetaxel-induced cytotoxicity and apoptosis by all-trans retinoic acid (ATRA) through downregulation of survivin (BIRC5), MCL-1 and LTbeta-R in hormone- and drug resistant prostate cancer cell line, DU-145. *J Exp Clin Cancer Res* 27: 37.
40. Chang HY, Sneddon JB, Alizadeh AA, Sood R, West RB, et al. (2004) Gene expression signature of fibroblast serum response predicts human cancer progression: similarities between tumors and wounds. *PLoS Biol* 2: E7.
41. Bittel DC, Kibiriyeva N, Sell SM, Strong TV, Butler MG (2007) Whole genome microarray analysis of gene expression in Prader-Willi syndrome. *Am J Med Genet A* 143: 430–442.

## Author Contributions

Conceived and designed the experiments: BM NC AP CM PG GT. Performed the experiments: BM NC ZH AP CM SP. Analyzed the data: BM AP CM JYT FF MP OG PG GT. Contributed reagents/materials/analysis tools: BM NC ZH SP MP OG PG GT. Wrote the paper: BM NC JYT FF MP OG PG GT. Responsible for the biological collection: SP MP OG PG GT. Quality controls: SP PG GT.



42. Schippert R, Schaeffel F, Feldkaemper MP (2008) Microarray analysis of retinal gene expression in chicks during imposed myopic defocus. *Mol Vis* 14: 1589–1599.
43. Huang da W, Sherman BT, Lempicki RA (2009) Systematic and integrative analysis of large gene lists using DAVID bioinformatics resources. *Nat Protoc* 4: 44–57.
44. Huang da W, Sherman BT, Lempicki RA (2009) Bioinformatics enrichment tools: paths toward the comprehensive functional analysis of large gene lists. *Nucleic Acids Res* 37: 1–13.
45. Computing RfIS (2012) R: A language and environment for statistical computing. In: Team RDC, editor. Vienna.
46. Kanehisa M, Goto S (2000) KEGG: kyoto encyclopedia of genes and genomes. *Nucleic Acids Res* 28: 27–30.
47. Kanehisa M, Goto S, Sato Y, Furumichi M, Tanabe M (2012) KEGG for integration and interpretation of large-scale molecular data sets. *Nucleic Acids Res* 40: D109–114.
48. Lanfranco MF, Seitz PK, Morabito MV, Emeson RB, Sanders-Bush E, et al. (2009) An innovative real-time PCR method to measure changes in RNA editing of the serotonin 2C receptor (5-HT<sub>2C</sub>R) in brain. *J Neurosci Methods* 179: 247–257.
49. Schefé JH, Lehmann KE, Buschmann IR, Unger T, Funke-Kaiser H (2006) Quantitative real-time RT-PCR data analysis: current concepts and the novel “gene expression’s CT difference” formula. *J Mol Med* 84: 901–910.
50. Livak KJ, Schmittgen TD (2001) Analysis of relative gene expression data using real-time quantitative PCR and the 2(-Delta Delta C(T)) Method. *Methods* 25: 402–408.
51. Wong ML, Medrano JF (2005) Real-time PCR for mRNA quantitation. *Biotechniques* 39: 75–85.
52. Bates S, Rowan S, Vousden KH (1996) Characterisation of human cyclin G1 and G2: DNA damage inducible genes. *Oncogene* 13: 1103–1109.
53. Xu G, Bernaldo S, Fu G, Lee DY, Yang BB, et al. (2008) Cyclin G2 is degraded through the ubiquitin-proteasome pathway and mediates the antiproliferative effect of activin receptor-like kinase 7. *Mol Biol Cell* 19: 4968–4979.
54. Choi MG, Noh JH, An JY, Hong SK, Park SB, et al. (2009) Expression levels of cyclin G2, but not cyclin E, correlate with gastric cancer progression. *J Surg Res* 157: 168–174.
55. Ohata N, Ito S, Yoshida A, Kunisada T, Numoto K, et al. (2006) Highly frequent allelic loss of chromosome 6q16-23 in osteosarcoma: involvement of cyclin C in osteosarcoma. *Int J Mol Med* 18: 1153–1158.
56. Miyata Y, Liu Y, Jankovic V, Sashida G, Lee JM, et al. (2010) Cyclin C regulates human hematopoietic stem/progenitor cell quiescence. *Stem Cells* 28: 308–317.
57. Wang L, Yin F, Du Y, Chen B, Liang S, et al. (2010) Depression of MAD2 inhibits apoptosis and increases proliferation and multidrug resistance in gastric cancer cells by regulating the activation of phosphorylated survivin. *Tumour Biol* 31: 225–232.
58. Matsuoka S, Edwards MC, Bai C, Parker S, Zhang P, et al. (1995) p57KIP2, a structurally distinct member of the p21CIP1 Cdk inhibitor family, is a candidate tumor suppressor gene. *Genes Dev* 9: 650–662.
59. Kang MA, Kim JT, Kim JH, Kim SY, Kim YH, et al. (2009) Upregulation of the cyclin kinase subunit CKS2 increases cell proliferation rate in gastric cancer. *J Cancer Res Clin Oncol* 135: 761–769.
60. Schwartz BE, Larochele S, Suter B, Lis JT (2003) Cdk7 is required for full activation of *Drosophila* heat shock genes and RNA polymerase II phosphorylation in vivo. *Mol Cell Biol* 23: 6876–6886.
61. Matsuno M, Kose H, Okabe M, Hiromi Y (2007) TFIIF controls developmentally-regulated cell cycle progression as a holocomplex. *Genes Cells* 12: 1289–1300.
62. Gentile A, Ditt RF, Dias FO, Da Silva MJ, Dornelas MC, et al. (2009) Characterization of ScMat1, a putative TFIIF subunit from sugarcane. *Plant Cell Rep* 28: 663–672.
63. Gladden AB, Diehl JA (2003) The cyclin D1-dependent kinase associates with the pre-replication complex and modulates RB/MCM7 binding. *J Biol Chem* 278: 9754–9760.
64. Mutch DM, Berger A, Mansourian R, Rytz A, Roberts MA (2002) The limit fold change model: a practical approach for selecting differentially expressed genes from microarray data. *BMC Bioinformatics* 3: 17.
65. Joyce NC, Zhu CC, Harris DL (2009) Relationship among oxidative stress, DNA damage, and proliferative capacity in human corneal endothelium. *Invest Ophthalmol Vis Sci* 50: 2116–2122.
66. He Z, Campolmi N, Ha Thi BM, Dumollard JM, Peoc’h M, et al. (2011) Optimization of immunolocalization of cell cycle proteins in human corneal endothelial cells. *Mol Vis* 17: 3494–3511.
67. Joyce NC, Meklir B, Joyce SJ, Zieske JD (1996) Cell cycle protein expression and proliferative status in human corneal cells. *Invest Ophthalmol Vis Sci* 37: 645–655.
68. Joyce NC, Harris DL, Zhu CC (2011) Age-related gene response of human corneal endothelium to oxidative stress and DNA damage. *Invest Ophthalmol Vis Sci* 52: 1641–1649.
69. Ikebe H, Takamatsu T, Itoi M, Fujita S (1984) Cytofluorometric nuclear DNA determinations on human corneal endothelial cells. *Exp Eye Res* 39: 497–504.
70. Ikebe H, Takamatsu T, Itoi M, Fujita S (1986) Age-dependent changes in nuclear DNA content and cell size of presumably normal human corneal endothelium. *Exp Eye Res* 43: 251–258.
71. Ikebe H, Takamatsu T, Itoi M, Fujita S (1988) Changes in nuclear DNA content and cell size of injured human corneal endothelium. *Exp Eye Res* 47: 205–215.
72. Joyce NC, Navon SE, Roy S, Zieske JD (1996) Expression of cell cycle-associated proteins in human and rabbit corneal endothelium in situ. *Invest Ophthalmol Vis Sci* 37: 1566–1575.
73. Kikuchi M, Harris DL, Obara Y, Senoo T, Joyce NC (2004) p27kip1 Antisense-induced proliferative activity of rat corneal endothelial cells. *Invest Ophthalmol Vis Sci* 45: 1763–1770.
74. Pagano M, Jackson PK (2004) Wagging the dogma; tissue-specific cell cycle control in the mouse embryo. *Cell* 118: 535–538.
75. Yokoi T, Seko Y, Makino H, Hatou S, Yamada M, et al. (2012) Establishment of functioning human corneal endothelial cell line with high growth potential. *PLoS one* 7: e29677.
76. Joyce NC (2005) Cell cycle status in human corneal endothelium. *Exp Eye Res* 81: 629–638.
77. Paull AC, Whikehart DR (2005) Expression of the p53 family of proteins in central and peripheral human corneal endothelial cells. *Mol Vis* 11: 328–334.
78. Song Z, Wang Y, Xie L, Zang X, Yin H (2008) Expression of senescence-related genes in human corneal endothelial cells. *Mol Vis* 14: 161–170.
79. Sardet C, Vidal M, Cobrinik D, Geng Y, Onufryk C, et al. (1995) E2F-4 and E2F-5, two members of the E2F family, are expressed in the early phases of the cell cycle. *Proc Natl Acad Sci U S A* 92: 2403–2407.
80. Liu L, Lee S, Zhang J, Peters SB, Hannah J, et al. (2009) CUL4A abrogation augments DNA damage response and protection against skin carcinogenesis. *Mol Cell* 34: 451–460.
81. Luo Y, Schwartz C, Shin S, Zeng X, Chen N, et al. (2006) A focused microarray to assess dopaminergic and glial cell differentiation from fetal tissue or embryonic stem cells. *Stem Cells* 24: 865–875.
82. Bao JJ, Le XF, Wang RY, Yuan J, Wang L, et al. (2002) Reexpression of the tumor suppressor gene ARHI induces apoptosis in ovarian and breast cancer cells through a caspase-independent calpain-dependent pathway. *Cancer Res* 62: 7264–7272.
83. Lu X, Qian J, Yu Y, Yang H, Li J (2009) Expression of the tumor suppressor ARHI inhibits the growth of pancreatic cancer cells by inducing G1 cell cycle arrest. *Oncol Rep* 22: 635–640.
84. Lee HT, Kay EP (2003) Regulatory role of PI 3-kinase on expression of Cdk4 and p27, nuclear localization of Cdk4, and phosphorylation of p27 in corneal endothelial cells. *Invest Ophthalmol Vis Sci* 44: 1521–1528.
85. Sugawara K (2009) UV-DDB: a molecular machine linking DNA repair with ubiquitination. *DNA Repair (Amst)* 8: 969–972.
86. Inoki T, Endo H, Inoki Y, Hamamoto T, Tsuru T, et al. (2004) Damaged DNA-binding protein 2 accelerates UV-damaged DNA repair in human corneal endothelium. *Exp Eye Res* 79: 367–376.
87. Joyce NC, Harris DL, Zieske JD (1998) Mitotic inhibition of corneal endothelium in neonatal rats. *Invest Ophthalmol Vis Sci* 39: 2572–2583.
88. Joyce NC, Harris DL, Mello DM (2002) Mechanisms of mitotic inhibition in corneal endothelium: contact inhibition and TGF-beta2. *Invest Ophthalmol Vis Sci* 43: 2152–2159.
89. Lee C, Cho Y (2002) Interactions of SV40 large T antigen and other viral proteins with retinoblastoma tumour suppressor. *Rev Med Virol* 12: 81–92.
90. LaCasse EC, Baird S, Korneluk RG, MacKenzie AE (1998) The inhibitors of apoptosis (IAPs) and their emerging role in cancer. *Oncogene* 17: 3247–3259.
91. Konomi K, Joyce NC (2007) Age and topographical comparison of telomere lengths in human corneal endothelial cells. *Mol Vis* 13: 1251–1258.
92. Wilson SE, Lloyd SA, He YG, McCash CS (1993) Extended life of human corneal endothelial cells transfected with the SV40 large T antigen. *Invest Ophthalmol Vis Sci* 34: 2112–2123.
93. Feldman ST, Gjerset R, Gately D, Chien KR, Feramisco JR (1993) Expression of SV40 virus large T antigen by recombinant adenoviruses activates proliferation of corneal endothelium in vitro. *J Clin Invest* 91: 1713–1720.
94. Wilson SE, Weng J, Blair S, He YG, Lloyd S (1995) Expression of E6/E7 or SV40 large T antigen-coding oncogenes in human corneal endothelial cells indicates regulated high-proliferative capacity. *Invest Ophthalmol Vis Sci* 36: 32–40.
95. Liu Z, Zhuang J, Li C, Wan P, Li N, et al. (2012) Long-term cultivation of human corneal endothelial cells by telomerase expression. *Exp Eye Res* 100: 40–51.
96. McAlister JC, Joyce NC, Harris DL, Ali RR, Larkin DF (2005) Induction of replication in human corneal endothelial cells by E2F2 transcription factor cDNA transfer. *Invest Ophthalmol Vis Sci* 46: 3597–3603.
97. Joyce NC, Harris DL (2010) Decreasing expression of the G1-phase inhibitors, p21Cip1 and p16INK4a, promotes division of corneal endothelial cells from older donors. *Mol Vis* 16: 897–906.
98. Fuchsluger TA, Jurkunas U, Kazlauskas A, Dana R (2011) Anti-apoptotic gene therapy prolongs survival of corneal endothelial cells during storage. *Gene Ther*.
99. Peh GS, Toh KP, Wu FY, Tan DT, Mehta JS (2011) Cultivation of human corneal endothelial cells isolated from paired donor corneas. *PLoS one* 6: e28310.

100. Shin YJ, Cho DY, Chung TY, Han SB, Hyon JY, et al. (2011) Rapamycin reduces reactive oxygen species in cultured human corneal endothelial cells. *Curr Eye Res* 36: 1116–1122.
101. Bayyoud T, Thaler S, Hofmann J, Maurus C, Spitzer MS, et al. (2012) Decellularized bovine corneal posterior lamellae as carrier matrix for cultivated human corneal endothelial cells. *Curr Eye Res* 37: 179–186.
102. Watanabe R, Hayashi R, Kimura Y, Tanaka Y, Kageyama T, et al. (2011) A novel gelatin hydrogel carrier sheet for corneal endothelial transplantation. *Tissue Eng Part A* 17: 2213–2219.
103. Senoo T, Obara Y, Joyce NC (2000) EDTA: a promoter of proliferation in human corneal endothelium. *Invest Ophthalmol Vis Sci* 41: 2930–2935.
104. Patel SP, Bourne WM (2009) Corneal endothelial cell proliferation: a function of cell density. *Invest Ophthalmol Vis Sci* 50: 2742–2746.
105. Senoo T, Joyce NC (2000) Cell cycle kinetics in corneal endothelium from old and young donors. *Invest Ophthalmol Vis Sci* 41: 660–667.
106. Yokoo S, Yamagami S, Yanagi Y, Uchida S, Mimura T, et al. (2005) Human corneal endothelial cell precursors isolated by sphere-forming assay. *Invest Ophthalmol Vis Sci* 46: 1626–1631.
107. Hatou S, Yoshida S, Higa K, Miyashita H, Inagaki E, et al. (2013) Functional corneal endothelium derived from corneal stroma stem cells of neural crest origin by retinoic acid and Wnt/beta-catenin signaling. *Stem Cells Dev* 22: 828–839.
108. Yu WY, Sheridan C, Grierson I, Mason S, Kearns V, et al. (2011) Progenitors for the corneal endothelium and trabecular meshwork: a potential source for personalized stem cell therapy in corneal endothelial diseases and glaucoma. *J Biomed Biotechnol* 2011: 412743.